STABILITY OF SUBMARINE SLOPES

GEO REPORT No. 47

N.C. Evans

This report was extracted from GEO Special Project
Report No. SPR 4/94, which was produced in June 1994

First published, June 1995

Prepared by:

Geotechnical Engineering Office,
Civil Engineering Department,
Civil Engineering Building,
101 Princess Margaret Road,
Homantin, Kowloon,
Hong Kong.

This publication is available from:

Government Publications Centre,
Ground Floor, Low Block,
Queensway Government Offices,
66 Queensway,
Hong Kong.

Overseas orders should be placed with:

Publications (Sales) Office,
Information Services Department,
28th Floor, Siu On Centre,
188 Lockhart Road, Wan Chai,
Hong Kong.

Price in Hong Kong: HK$46
Price overseas: US$8.5 (including surface postage)

An additional bank charge of **HK$50** or **US$6.50** is required per cheque made in currencies other than Hong Kong dollars.

Cheques, bank drafts or money orders
must be made payable to **HONG KONG GOVERNMENT**

PREFACE

In keeping with our policy of releasing information of general technical interest, we make available some of our internal reports in a series of publications termed the GEO Report series. The reports in this series, of which this is one, are selected from a wide range of reports produced by the staff of the Office and our consultants.

Copies of GEO Reports have previously been made available free of charge in limited numbers. The demand for the reports in this series has increased greatly, necessitating new arrangements for supply. Henceforward a charge will be made to cover the cost of printing.

The Geotechnical Engineering Office also publishes guidance documents and presents the results of research work of general interest in GEO Publications. These publications and the GEO Reports may be obtained from the Government's Information Services Department. Information on how to purchase these publications is given on the last page of this report.

A. W. Malone
Principal Government Geotechnical Engineer
June 1995

FOREWORD

This report presents a comprehensive review of overseas literature on the stability of submarine slopes and the application of analytical techniques to typical submarine slopes in Hong Kong waters. Two main types of slope have been considered, namely, natural seabed slopes and dredged slopes (cut slopes).

The report was prepared by N.C. Evans under the general direction of Dr J. Premchitt. The report forms part of the on-going study of marine geotechnology topics relevant to the implementation of the Port and Airport Development Strategy (PADS).

Y.C. Chan
Chief Geotechnical Engineer/Special Projects

CONTENTS

		Page No.
	Title Page	1
	PREFACE	3
	FOREWORD	4
	CONTENTS	5
1.	INTRODUCTION	7
2.	BACKGROUND	7
	2.1 Generic Types of Submarine Instability	7
	2.2 Morphological Types of Submarine Instabilities	8
	2.2.1 Peripheral Rotational Slumps	8
	2.2.2 Collapse Depressions	9
	2.2.3 Bottleneck Slides	9
	2.2.4 Elongated Retrogressive Slides and Mudflow Gullies	9
	2.3 Structural Features Associated with Seabed Failures	9
	2.4 Mechanisms of Submarine Instability	9
	2.4.1 Gravitational Forces	9
	2.4.2 Hydraulic Forces	10
	2.4.3 Seismic Forces	10
	2.5 Strength of Seabed Soils	10
	2.5.1 Cohesive Soils	10
	2.5.2 Granular Soils	10
	2.6 Cyclic Loading of Seabed Soils	11
	2.7 Oceanographic Considerations	12
3.	STABILITY ANALYSES	13
	3.1 Stability under Gravitational Forces	13
	3.2 Creep	14
	3.3 Stability under Wave Forces	14
	3.4 Stability under Seismic Forces	15

		Page No.
	3.5 Stress-relief Effects	15
	3.6 High-mobility Failures	16
	3.6.1 Mudflows	16
	3.6.2 Turbidity Currents	17
	3.7 Run-out Distances	17
4.	HONG KONG - REGIONAL FACTORS	17
	4.1 Introduction	17
	4.2 Water Circulation Patterns	18
	4.3 Depositional Environments	18
	4.4 Sedimentation Rates and Geotechnical Properties	19
	4.5 Pearl River Mouth Continental Shelf Seabed Instabilities	20
	4.5.1 Quaternary Sea-level Change	20
	4.5.2 Seismicity	20
	4.6 Submarine Slope Stability in Hong Kong Waters	20
5.	NATURAL SLOPES, NORTH LANTAU	21
	5.1 Study Area	21
	5.2 Natural Slopes	21
	5.3 Theoretical Model	22
6.	DREDGED SLOPES, PLOVER COVE	23
7.	DREDGED SLOPES, URMSTON ROAD	23
	7.1 Geotechnical Characteristics	24
	7.2 Oceanographic Characteristics	24
	7.3 Stability	24
8.	CONCLUSIONS	25
9.	REFERENCES	26
	LIST OF FIGURES	31

1. INTRODUCTION

The developments comprising the new airport at Chek Lap Kok and the various Port and Airport Development Strategy (PADS) projects involve massive marine civil engineering works, the locations of which are further offshore and more exposed than has previously been the case in Hong Kong. The behaviour of the seabed soils is an important factor in the design and performance of the works. This report examines submarine slope stability in Hong Kong, and addresses both the theoretical background to the subject and the actual seabed conditions in Hong Kong and adjacent waters.

Section 2 provides a general introduction and outlines the factors that could affect submarine slope stability, while Section 3 reviews submarine slope stability theories. Section 4 looks at the sea bed in Hong Kong in a regional context, describing the water circulation patterns and depositional environments in the area, and examining the probable impacts of these regional factors on submarine slope stability.

Section 5 examines the stability of natural submarine slopes off North Lantau and proposes a theoretical model explaining the seabed topography in this area, while Sections 6 and 7 examine the stability of dredged slopes in Plover Cove and Urmston Road respectively, comparing stability predictions with measured slope data. Conclusions are presented in Section 8.

2. BACKGROUND

2.1 Generic Types of Submarine Instability

Moore (1978) classified submarine slope failures into three general generic categories, as follows:

(a) Slides in recent deposits of weak, under-consolidated, metastable soils in areas of rapid sedimentation, such as delta fronts or submarine canyon heads. These slides often take the form of "collapse slumps". Undrained failures may be initiated directly by dynamic (seismic or hydraulic) forces. There are many published works concerning the description and analysis of this type of failure, most of which are based on research in the Mississippi River Delta, USA, e.g. Coleman and Prior (1978), Coleman and Garrison (1977), Booth and Garrison (1978), Bea et al (1983) and Prior and Coleman (1978).

(b) Slides in older, probably normally consolidated sediments triggered by significant changes in the sedimentary and erosional regimes which may be caused by sea level changes or migration of erosional channels. Sudden increases in deposition can cause undrained or partially-drained failures, while erosional oversteepening can trigger drained failures.

(c) Slides in older, probably normally consolidated sediments caused by tectonic processes, such as earthquakes or oversteepening by tectonic uplift. Instabilities associated with tectonic forces were described by Morin and Pereira (1987) from the Grand Banks of Newfoundland, and by Almagor et al (1984) from the

USA Mid-Atlantic margin.

To Moore's three categories we propose adding a fourth as follows:

(d) Slides triggered by engineering works such as excavation, dumping, or alteration of the hydraulic regime with resulting scour or increased deposition. Applying a surcharge to existing slopes may also induce failure. Oversteepening by excavation, scour/increased deposition, or dumping may lead directly to failure from gravitational forces, the type of failure depending on the rate of excavation and the permeability of the sediments. Oversteepening will also increase the vulnerability of a slope to wave or seismic forces. Slides in dumped materials are in some ways analogous to category (a) slides as dumped spoil may be weak, under-consolidated and metastable.

The seabed soils of Hong Kong are generally normally consolidated, the erosional/depositional environment is mild over much of the Territory and the area is regarded as having low seismicity. The natural seabed slope forms in Hong Kong are generally stable and are in equilibrium with long term hydraulic and seismic forces. Of the above four categories of submarine failure only (d) - failure due to engineering works - can be considered to be of immediate importance. However, category (a) - failure of weak, under-consolidated sediments - also merits attention due to Hong Kong's proximity to the dynamic environment of the Pearl River.

2.2 Morphological Types of Submarine Instabilities

Denlinger and Iverson (1990) examined the boundary conditions at the slope surface for the submarine condition and concluded that, under conditions of steady seepage, submarine slopes always undergo Coulomb failure prior to liquefaction. However, if slope angles are low, submarine slopes are close to a liquefied state when failure occurs. This favours long landslide runouts and sediment flow subsequent to failure.

Surface failures in weak, under-consolidated, deltaic deposits have been described by Coleman and Prior (1978) from the Mississippi River Delta. Coleman and Prior distinguished between the following major categories, which are illustrated schematically in Figures 1 and 2.

2.2.1 Peripheral Rotational Slumps

Generally these have a well-defined scarp and a curved or curvilinear plan form. The slumped mass is normally hummocky with irregular topography. Multiple shear planes merge at depth into a single basal shear surface parallel to the sedimentary bedding. Lateral movements may reach 1,000 m. The failure trigger is thought to be depositional oversteepening with excess pore pressures and under-consolidation.

2.2.2 Collapse Depressions

Bowl-shaped depressions which are surrounded by distinct scarps. The sediments involved are usually soft organic clays containing large amounts of methane gas. Diameters range from 50 m to 150 m and the scarps may exceed 3 m in height. The central area displays irregular and hummocky topography. These features are thought to arise from volumetric changes associated with the rapid loss of methane gas and pore water. During failure the soils would be liquified and would not support any load. Storm waves may trigger the collapse.

2.2.3 Bottleneck Slides

These are similar to collapse depressions except that on the downslope side, the debris spills out onto the surrounding stable sediments. The slide length may be up to 600 m.

2.2.4 Elongated Retrogressive Slides and Mudflow Gullies

These features have been found in water depths of 10 m to 100 m. Most have a recognisable rotational head slump at their upslope margins and their morphology compares closely to that of terrestrial mudslides and mudflows. These features have been measured at over 10km in length, and comprise a long narrow channel linking a depressed source area to lobes or fans downslope. These slides are thought to begin as bottleneck slides, with channels developing as a direct result of the loading of the surrounding slopes by discharged debris, which generates high pore pressures and a loss of strength in the underlying spoil. The failure can continue on slopes that are shallower than those on which the initial bottleneck slide occurred. Morgenstern (1967) described a similar process which he refers to as "collapse slumping".

2.3 Structural Features Associated with Seabed Failures.

Watkins and Kraft (1976) summarised deformational slide features that can be identified from the examination of high-resolution geophysical records. Twelve types of structural feature were found and these are illustrated in Figures 3 to 5.

2.4 Mechanisms of Submarine Instability

There appear to be three main driving mechanisms causing submarine instability in continental shelf areas, and these have been summarised by Poulos (1988) as follows.

2.4.1 Gravitational Forces

Soil movements due to gravitational loading (other than consolidation settlements) may be categorised as either instability or creep phenomena. Instability occurs when stresses in the seafloor soils equal or exceed the available shear strength, causing sudden movement.

Creep under constant stress may occur in cohesive soils, resulting in slow but persistent movement over a long period of time.

2.4.2 Hydraulic Forces

Hydraulic forces affecting the seafloor result from currents, tides and surface waves. Large surface waves affect stability by applying cyclic bottom pressures to the seafloor. The amplitude and frequency of the induced bottom pressure depends on the soil properties, the height and wavelength of the surface waves, and the mean water depth. Bottom pressures under severe storm waves may be sufficient to trigger shear failures in soft sediments where water depths are less than about 120 m (Henkel, 1970). The failure of offshore oil platform foundations in 100 m of water in the Gulf of Mexico has been shown to be the result of bottom movements caused by the passage of hurricane-induced surface waves (Bea and Wright, 1983). Tides and currents will tend to have a more indirect effect on submarine stability, whereby erosional and depositional processes may lead to the undercutting or overloading of existing slopes. Any change in tidal or current regime may have an adverse impact on submarine slope stability by altering the seabed topography. It should be noted that many currents comprise wind-induced surface drift only and do not contribute to bottom-scouring processes.

2.4.3 Seismic Forces

The main effect of earthquakes on submarine stability is the development of horizontal travelling waves in the bedrock under the soil deposits. Vertical propagation of these waves to the soil surface induces cyclic shear stresses in the soil. These stresses can result in significant lateral strains and strength losses within the soils which, alone or in conjunction with gravitational and hydraulic forces, may lead to slope failure.

2.5 Strength of Seabed Soils

2.5.1 Cohesive Soils

It is conventional to express the strength of cohesive marine soils by using the normalised stress ratio c_u/σ'_{vo}, where c_u is the undrained shear strength and σ'_{vo} is the effective overburden stress. This ratio is extensively used in submarine stability analyses and reflects the overall strength and consolidation state of the sediments. Morgenstern (1967) presented an almost straight line relation between c_u/σ'_{vo} and Plasticity Index for normally consolidated soils, as shown in Figure 6. Significant deviations from this trend suggest the presence either of diagenetic bonding (cementation) and associated strength gain, or under-consolidation with associated strength loss. For most normally consolidated soils c_u/σ'_{vo} values fall in the range 0.20 to 0.45. Insitu Hong Kong cohesive marine soils are in this range.

2.5.2 Granular Soils

The strength of a granular submarine soil may be typified by the effective friction angle, which depends on both the mineralogy of the deposit and its relative density. It can be shown that a submerged slope in granular materials will, in the absence of internal seepage forces or external loads, stand at an angle of ϕ'_{max}, (Lambe and Whitman, 1979) where ϕ'_{max} is a function of the critical shearing angle and the dilatancy.

The critical shearing angle is the friction angle at which dilation becomes zero and the material reaches a critical state. The critical friction angle, ϕ'_{crit}, may be assessed from simple shear tests or, approximately (to $\pm$ 1 degree), from the angle of repose of loose dry sand (Bolton, 1986). The critical friction angle is partly dependent on mineralogy and has been observed to range from 32 degrees in quartz sands to perhaps 40 degrees in feldspathic sands. Bolton suggested that if a ϕ'_{crit} of 33 degrees is assumed for a predominantly quartz sand the maximum error involved is likely to be 1 to 2 degrees. Dilation may be assessed by theoretical methods (Rowe, 1962 and 1969, De Josselin de Jong, 1976). Bolton (1986) demonstrated that if the relative density and mean effective stress are known an estimate may be made of the maximum dilation angle and of ϕ'_{max}.

Relative density may be very approximately estimated from SPT N values, or alternatively may be calculated by comparison of measured bulk densities with minimum and maximum densities determined in the laboratory. Accurate determination of insitu bulk density from "undisturbed" samples is, however, problematic and some authors suggest that sample densification during sampling and handling may lead to overestimates of the relative density. If bulk density measurements are made they should be performed on board the drilling vessel almost immediately after sampling to prevent sample deterioration. Relative density may also be assessed from CPT data (Schmertmann, 1975 and Lunne and Christoffersen, 1983).

On completion of dredging the slope stability will depend initially upon the peak strength (ϕ'_{max}). Bolton (1986) made the important point that all ϕ'_{max} values in excess of ϕ'_{crit} are transitory if large strains occur, and that design calculations using ϕ'_{max} demand further assurance that a progressive failure will not occur.

2.6 Cyclic Loading of Seabed Soils

The residual pore-pressure generated in a seabed soil by cyclic wave-induced bottom pressures is dependant on the nature and stress history of the soil. Prediction of soil and pore-pressure response in these circumstances is complex and has been approached, by various authors, by numerical or critical-state techniques (e.g. Lo & Lee, 1973, Hyde & Ward, 1985). However, it is now commonly recognised that the behaviour of sands and clays under cyclic loading is fundamentally similar, and the following general points may be made. Undrained cyclic loading of saturated contractive soils results in an accumulation of positive excess residual pore pressure with associated accumulation of strain. For both sands and clays the cyclic loading leads to failure when the cyclic limit state for the soil is reached. Sangrey et al (1978) reviewed this subject and came to the following conclusions.

Laboratory data indicate that the cyclic limit state coincides with the remoulded strength state for clays and the steady state for sands, while it is also probable that the undrained shear strength of a contractive clay after cyclic loading is approximately equal to the monotonic shear strength. Liquefaction of sands is a special case within the more general category of strength reduction of contractive soils.

Undrained cyclic loading of saturated dilative soils will tend to reduce pore pressures. Dilative sands will tend to initially accumulate positive residual pore pressures during cyclic loading, but strength reductions are not usually significant. Succeeding cycles will reduce pore pressures as the sand dilates, and the soil will stiffen. Significant strains ("cyclic mobility") may be generated by further cycles as the pore pressure again increases, but failure by liquefaction will not occur under these circumstances. Subsequent monotonic loading may show undrained compressive strengths to be approximately the same as before cyclic loading.

Drainage of a contractive clay under cyclic loading will tend to dissipate the generated positive pore pressures, with a reduction in void ratio and water content and a subsequent increase in undrained shear strength. The relationship between the final shear strength and the shear strength prior to cyclic loading will depend upon the clay sensitivity and the magnitude of the void ratio reduction. Similarly, drainage of a contractive sand during cyclic loading will tend to reduce the pore pressure build up and will improve liquefaction resistance.

Under drained conditions a dilative clay under cyclic loading will allow lowered pore pressures to recover, with consequent increases in void ratio and water content and a decrease in undrained shear strength. Similarly, under drained conditions a dilative sand during cyclic loading will permit lowered pore pressures to recover with a subsequent loss of stiffness.

2.7 Oceanographic Considerations

When examining the effects of seafloor pressures induced by surface waves, the selection of appropriate characteristics for the "design wave" is an important part of the analytical process. The wave parameters generally used in slope stability calculations are wave height, H, and wavelength, L, which are linked by wave period, T, and wave velocity, C. It is possible to establish the following parameters from recorded wave data (US Army Corps of Engineers, 1984) :

H_{max} the greatest recorded height from trough to adjacent crest.

H_S the significant wave height, defined as the mean height of the highest 1/3 of all waves.

H_O the deepwater wave height (no shoaling influence).

H_{10} the mean height of the highest 10% of all waves.

H_1 the mean height of the highest 1% of all waves.

T_S the period associated with H_S.

T_P the period corresponding to the peak of the wave energy spectrum.

Statistical analysis of historical measured wave data allows the return periods of waves of given parameter values to be estimated. For sites where recorded wave data are not available, estimations of wave conditions must be made. Under these circumstances wave characteristics are usually determined for deep water and then corrected for shorewards propagation (US Army Corps of Engineers, 1984). Deepwater wave height, H_0, and significant wave period, T_S, may be determined if wind speed, wind duration and fetch length data are available. This information, with water level data, is used to perform refraction, diffraction and shoaling analyses to determine wave conditions at the site. Once wave characteristics at a site have been estimated, further analyses may be performed to determine whether wave breaking can occur or not and to assess the effect of wave breaking on wave heights. The height at which a wave breaks is influenced both by the wave characteristics and by the depth and topography of the seabed.

For non-breaking waves the design wave height is selected from the statistical height distributions. The corresponding wavelength may be determined from various design charts. Guidelines for the analysis of marine structures suggest that H_1 is used for rigid structures, H_1 to H_{10} for semirigid structures and H_5 to H_S for flexible structures (US Army Corps of Engineers, 1984). Generally-accepted guidelines for design wave heights for submarine slopes have not yet been established. For critical slopes it may be advisable to use H_{max} for all analyses (Nataraja & Gill, 1983).

3. STABILITY ANALYSES

3.1 Stability under Gravitational Forces

Methods of analysing the stability of terrestrial slopes subject to gravitational forces are well known. Most such techniques are based on limit-equilibrium methods (eg: Bishop, 1955 or Janbu, 1973). These methods generally require detailed data on pore pressures, which are not usually available for submarine slopes. Morgenstern (1967) examined this problem and concluded that for submarine slopes, which are often relatively gentle and extensive, a simple infinite slope analysis is generally adequate. Analyses for undrained and drained stability are reviewed in Evans (1992). The factor of safety of a cohesive submarine soil slope under gravitational loads may be calculated as follows (after Poulos, 1988) :

$$F = \frac{2}{\sin 2\alpha} \left(\frac{c_u}{\sigma'_{vo}} \right) \quad \ldots\ldots\ldots\ldots\ldots \quad (1)$$

where F = factor of safety
α = slope angle
c_u = undrained shear strength
σ'_{vo} = effective overburden pressure

In certain circumstances a partly drained condition may exist within submarine soil slopes, with the existence of excess pore pressures. Such pressures may be caused by rapid deposition and under-consolidation, a situation in which the soil particles are partly supported by the pore-water, or by the generation of gas within the soil. Poulos (1988) has summarised an effective stress method for calculating the stability of accreting fine sediments using the method of Gibson (1958) to estimate the approximate excess pore pressures.

For drained conditions in a normally-consolidated clay or uncemented sand or silt with c' approximately zero (after Lambe & Whitman, 1979) :

$$F = \frac{\tan\phi'}{\tan\alpha} \quad \ldots\ldots\ldots\ldots\ldots\ldots \quad (2)$$

where ϕ' = effective friction angle
α = slope angle

3.2 Creep

Creep may be defined as the slow downslope movement of sediment under gravity. The process may be significant on submarine slopes where relatively low stresses exist over long periods of time. Creep may also be a precursor to slope failure due to strength degradation through accumulating strains or localised creep rupture. As creep processes are slow it would seem logical to analyse them under drained conditions (Booth et al 1984).

Singh and Mitchell (1968) developed an empirical creep parameter, m, which is the absolute value of the gradient of the line where log strain rate is plotted against log time. These data may be derived from drained triaxial creep tests. Booth et al (1984) showed that for a normally consolidated marine clay from the northeast USA, creep potential decreased with increasing consolidation stress, and the highest creep potential occurred at approximately the preconsolidation stress.

Booth et al (1984) described a mathematical process whereby downslope displacements may be calculated, and applied the analysis to submarine slopes off the northeast USA, with m=1.56, and predicted creep displacements ranging from 0.03 m/year for slopes of 5 degrees to 0.5 m/year for slopes of 10 degrees, with sediment thicknesses of 50 m. The equivalent predicted displacements for sediments of 20 m thickness were <0.01 m/year and 0.01 m/year for slopes of 5 degrees and 10 degrees respectively.

3.3 Stability under Wave Forces

Bottom pressures induced on the seafloor by wave action cause stress within the seafloor materials. These stresses in turn induce both transient and residual pore pressure changes, which affect the strength of the sediments and the stability of submarine slopes. Pore pressure changes due to wave action can result in the failure of cohesive soils and the liquefaction of sandy or silty material. Calculation of wave-induced bottom pressures and shear stresses, and their effects on cohesive seabed soils, are discussed in Evans (1992). The amplitude of wave pressure on the seafloor is given (after Poulos, 1988) by :

$$p_o = \frac{\gamma_W H}{2\cosh \Gamma h} \quad \ldots\ldots\ldots\ldots\ldots\ldots \quad (3)$$

where γ_W = unit weight of water
H = wave height
h = water depth

Γ = wave number = $2\pi/L$
L = wavelength

For granular seabed soils, any analysis must consider the potential for liquefaction under cyclic loads. The reader is referred to Pun (1992) for more detailed information on this subject. Nataraja and Gill (1983) made the point that sophisticated wave-induced liquefaction analyses, involving state-of-the-art analytical techniques with associated detailed field and laboratory investigations, are usually employed for very large, complex and capital-intensive marine works, but that such elaborate analyses are not warranted for smaller, less sensitive projects. Nataraja and Gill suggested a simplified analysis using SPT test results as described in Evans and Premchitt (1991). Isihara and Yamazaki (1984) proposed a technique fundamentally similar to that of Nataraja and Gill, although relative density is used to evaluate liquefaction resistance rather than SPT N values.

3.4 Stability under Seismic Forces

The stability of cohesive submarine slopes subjected to seismic forces is discussed in Evans (1992). Stability may be assessed as follows (after Morgenstern, 1967) :

$$\frac{c_u}{\sigma'_{vo}} = (0.5 \sin 2\alpha + k \cos^2\alpha \ \gamma/\gamma') \quad \ldots\ldots\ldots\ldots \quad (4)$$

where α = slope angle
k = seismic force as fraction of gravity
γ/γ' = approximately 3 for typical Hong Kong marine muds

For contractive granular submarine soils, partly drained or undrained cyclic loading may result in liquefaction. Simplified methods of evaluating liquefaction potential under earthquake loading have been presented by Seed and Idriss (1971), Isihara (1977), Iwasaki et al (1984), Seed et al (1983, 1984) and Robertson and Campanella (1985). These papers are summarised by Poulos (1988). Pun (1992) also examines this subject.

For preliminary evaluations of liquefaction potential under seismic loading, techniques using data from in-situ penetration tests are usually adequate. The general approach is to estimate the induced cyclic shear stress within the soil profile and compare it with the cyclic shear strength. Where the induced stress exceeds the strength there is potential for liquefaction.

3.5 Stress-relief Effects

Stress-relief effects on cohesive submarine slopes are discussed in Evans (1992). Stress relief effects in granular submarine soils are of interest in dredging operations. It has long been recognised that the stability of a sand slope being actively regressed by dredging is enhanced by the reduction of pore pressures from stress relief and dilatancy effects (Meijer and van Os, 1976, van Leussen and Nieuwenhuis, 1984). Stress relief, by elastic rebound of the soil skeleton, will have a small effect but the greatest component of pore pressure change is due to dilatancy of the sand as a result of shear forces induced within the slope by gravity. The reduction of pore pressure increases the effective stress in the soil so allowing the slope to stand at angles that would not otherwise be possible.

The rate at which the pore pressure regains its normal value - a function of the permeability of the soil - determines the speed at which the moving slope can be progressed, ie: as the pore pressures increase to normal values the soil strength decreases and the material becomes more dredgable. As an example, the rate of dredging in dense fine sands is low when using pure suction dredgers due to high dilatancy (which causes a large reduction in pore pressures) and low permeability (which results in slow pore pressure recovery). Hence cutter-suction dredgers are generally used in these types of material. Meijer and van Os (1976) reported that the inclination of an active dredging slope in fine sands may be up to 90 degrees without sliding taking place.

It is possible to analyse the forces involved using numerical methods and to predict the induced pore pressures (Meijer and van Os, 1976). As the stability of the receding slope is essentially transient, it may be considered more productive to examine the stability of the slope after completion of dredging. Once lowered pore pressures generated by the dredging process have recovered, the stability of the slope, in the absence of external dynamic forces, will be a function of the operative friction angle. Recovery of lowered pore pressures in even very fine sands can be expected to be relatively rapid and, in the case of sands with a high permeability, to be almost immediate.

3.6 High-mobility Failures

3.6.1 Mudflows

Submarine slope failures may, under certain circumstances, initiate flow slides that have the potential to travel relatively large distances on shallow gradients. Prior and Suhayda (1979) reported submarine mudflows from the Mississippi River Delta on slope angles of 0.5 to 1.7 degrees, while Lewis (1971) reported similar failures in slopes of 1 to 4 degrees off New Zealand. Prior and Coleman (1978) described such features from the Mississippi River Delta as "disintegrating retrogressive landslides" and cite parallels with terrestrial flow slides. Morgenstern (1967) referred to such phenomena under the title of "collapse slumping", and discussed a possible instability mechanism whereby an initial failure causes increases in pore pressures and loss of shear strength. Morgenstern suggests that such failures may occur in metastable materials such as those resulting from the accumulation of fine sediments.

Vallejo (1981) considered that the initial failure is generally of the shallow rotational or translational form and may be caused by dynamic effects, eg: wave action. A streaming condition then develops, usually travelling on a surface of low inclination. Vallejo analysed these flows and demonstrated that the factor of safety, F, against mudflow mobilisation can be examined as a special case of Equation (1), with the substitution of $2/\sin 2\alpha$ by $1/\alpha$ (in radians). The two expressions are nearly the same at small values of α. Vallejo's mudflow model is shown diagrammatically in Figure 7.

3.6.2 Turbidity Currents

Morgenstern (1967) examined the circumstances under which a submarine failure or mudflow could achieve greater mobility and could, in extreme cases, be transformed into a turbidity current. The following conclusions were reached. Slumps in stable cohesive sediments probably involve shearing on a plane or planes while the mass of sediment remains relatively intact. However, cohesive soils of high sensitivity and cohesionless soils, particularly metastable ones, have the potential to lose coherence during flow and to disperse rapidly. This is a situation that may arise in under-consolidated accumulating fine sediments. The process of transformation into a turbidity current involves the onset of turbulence and some mixing with overlying water. Among the factors that would deter a slump from transforming into a turbidity current are rapid decreases in slope gradient, and the dissipation of excess pore pressures. Thicker slumps will therefore transform more readily because the dissipation of pore pressure will be less.

3.7 Run-out Distances

Edgars and Karlsrud (1982) reviewed available data from published case histories of submarine slides and were able to show that the upper limit for run-out distance is related to the volume of the slide. The relationship is shown in graphical form in Figure 8. Edgars and Karlsrud also examined the possibility of using viscous flow analysis for submarine slides, but found that while the analysis could model observed run-outs very well using back-analysed parameters, there were difficulties in selecting input parameters to describe the viscous behaviour of soil.

4. HONG KONG - REGIONAL FACTORS

4.1 Introduction

Hong Kong is situated on the South China coast on the eastern side of the Pearl River estuary. The South China coast forms part of a stable landmass which was not subjected during the Pleistocene to subsidence, uplift or glaciation. Sea level changes have, however, resulted in the formation of the present topography which comprises a drowned coast bordered by hills of decomposed igneous rock (Lumb, 1977).

Hong Kong owes its existence as a major deep-water port to the fact that, despite close proximity to the sediment-laden Pearl River, sedimentation rates are very low. The limited requirement for maintenance dredging in Hong Kong waters is in marked contrast to the situation in Macau, where high sedimentation rates lead to constant problems in maintaining port facilities.

This section of the report examines the regional factors that result in these two very different sedimentary regimes existing in close proximity, and reaches some conclusions regarding the nature of possible seabed instabilities in Hong Kong and adjacent waters. The nature and geotechnical properties of the bottom sediments and the topography of the seabed, which have a major influence on the stability of submarine slopes, are partly dependent on the prevailing sedimentary regimes.

4.2 Water Circulation Patterns

Chalmers (1984) discussed mathematical modelling of Victoria Harbour and adjacent areas carried out by Hydraulics Research and the Water Research Centre (1983). This work predicts that dry season net tidal flows at North Lantau (Kap Shui Mun) and Lei Yue Mun are to the west, ie: there is an overall movement of water through Hong Kong from east to west. During the wet season an increase in freshwater flow from the Pearl River causes stratification in the water column, with a net seaward (easterly) flow of freshwater over a net landward (westerly) flow of denser salt water. Chalmers concludes that the average residual flow near the seabed at Lei Yue Mun and Kap Shui Mun probably remains westerly during the wet season, but does not offer evidence for this.

Kirby (1991) extended the above model to take account of Hong Kong's regional setting. Kirby suggested that while currents in Hong Kong are predominantly tidal, a progressive component is introduced by Coriolis circulation in the Pearl River estuary, and this tends to draw oceanic water from the east through Hong Kong and into the Pearl River via Tathong Channel, East Lamma Channel and Lantau Channel. This westerly drift is enhanced during the dry season by the WSW oceanic surface current induced by the northeast monsoon. Kirby agreed with Chalmers that a strong westerly near-bed residual current is maintained even during the wet season. Current measurements are being made for a number of ongoing projects, and should result in an increase of knowledge concerning the water circulation patterns in Hong Kong.

The above circulation model explains many aspects of the sedimentary regimes in the Hong Kong region, with oceanic water of low turbidity being drawn through the Territory from the east, while the sediment-rich waters of the Pearl River discharge down the western side of the estuary.

4.3 Depositional Environments

The Holocene marine sediments of Hong Kong primarily consist of the Hang Hau Formation (Strange & Shaw, 1986), a soft to very soft olive grey shelly mud (clayey silt or silty clay). These soils originated as a marine sequence deposited as sea level rose after the last glaciation. The rate of deposition of these materials and the present rate of sedimentation is pertinent to the strength and stability of the seabed.

Chalmers (1984) examined sedimentation in Victoria Harbour and concluded that there was a net accumulation of perhaps one million cu m per year of sediment, comprising sewage solids, dredging and reclamation spoil and Pearl River sediments. Kirby (1991) stated that the majority of this material is local sewage. Studies at Hong Kong University by Dr M. Peart suggest that natural fluvial inputs from Hong Kong rivers and streams are very small. The assumed net westerly flow of clear oceanic water through Hong Kong suggests that any Pearl River sediment entering through Kap Shui Mun on the ebb tide probably flows out again on the next flood tide, taking some of the locally-derived sediment with it.

Chalmers (1984) examined hydrographic data from Admiralty charts dating back to 1903 and found no evidence of persistent net sedimentation within Victoria Harbour. The relatively small maintenance dredging requirement tends to support this. Chalmers (1984) suggested that a situation exists whereby the seabed elevation is in dynamic equilibrium with the sea level, and that net sedimentation rates within Hong Kong waters have been determined by the Holocene rise in sea level from the low point of 120-150 m below present levels some 20,000 years ago. This model suggests that net natural deposition or erosion will only occur at times of sea level rise or fall respectively, or if the hydrodynamic regime is altered in any way. Chalmers suggests that occasional incursions of sediment-rich Pearl River water do enter Hong Kong under exceptional circumstances, and that these rare events are responsible for much of the sedimentation that does occur. The dynamic equilibrium theory would suggest that material deposited in this way will be later removed by wave and current action and will probably migrate westwards back towards the Pearl River.

Kirby (1991) agreed with the conclusion of Chalmers that there is very little net input of modern sediment to Hong Kong waters, and further concluded that the suspended load in Hong Kong is almost invariably very minor, with the muddy bed deposits being very stable and experiencing negligible change.

Recent work on the environmental impacts of dredging and dumping activities has, however, shown that the true situation may be a little more complex than this. A seabed sediment profiling camera survey, undertaken by Science Applications International Corporation of the USA, has shown that over much of Hong Kong the upper layers of the muddy seabed deposits (the top few cm or tens of cm) may, in fact, be highly mobile (Science Applications International Corporation, 1994). This survey was carried out in October 1993, after a sequence of storms had passed through Hong Kong, and the results may not be representative of the generally prevailing conditions. Further work is planned.

If the surface layers of the seabed deposits are highly mobile, this would tend to support the dynamic equilibrium theory, as the seabed topography appears to be relatively stable. It may be more realistic to consider the stability of seabed forms rather than of the seabed materials.

In marked contrast to the Hong Kong area, the western side of the Pearl estuary is a highly dynamic, unstable and high suspended solids regime (Kirby, 1991). The river discharge is strongly seasonal and the turbidity maximum migrates long distances between the wet and dry seasons. Tidal velocities vary greatly between subsequent tides due to the marked diurnal inequalities. Much of the estuary bed in the Macau region is thought to be floored by fluid muds. Pearl River suspended solids concentrations are typically 100 to 1,000 times greater than those of Hong Kong waters. Figure 9, derived from Evans (1988) and Li & Wang (1985) illustrates the general pattern of sediment distribution within the Pearl estuary and Hong Kong, showing how the active delta front is confined to the western shoreline.

4.4 Sedimentation Rates and Geotechnical Properties

Radiocarbon dating of Hong Kong sediments has shown that net deposition in the inshore areas began about 8,000 years ago (Yim, 1983). There is evidence that sea level rise has not been continuous, but has been interrupted by occasional regressions and erosive episodes, preserved in the sequence as gullied and oxidised horizons. If the dynamic equilibrium model of Chalmers (1984) is accepted, net sedimentation rates can be related to the rate of sea level rise. Local depositional episodes resulting from modern Pearl River sediment incursions are likely to have had only a transitory influence.

A relatively slow rate of net deposition, related to the rate of sea level rise, suggests that under- or over-consolidation will not have occurred. Lumb (1977) examined the geotechnical properties of the marine soils of Hong Kong and concluded that all were normally consolidated. Lumb quotes c_u/σ_{vo}' values of 0.22 to 0.39 for muds from various locations, and attributes strength variations to sulphate content.

4.5 Pearl River Mouth Continental Shelf Seabed Instabilities

Li and Jin (1989) presented a review of seafloor instabilities on the continental shelf in the Pearl River Mouth Basin, based on high resolution seismic reflection data. Shallow faults, gassy sediments and mud diapirs were noted. Shallow faults appeared to be most common in water depths of 30 m to 80 m. Displacements are generally in the range of several to over 10 m. Gas-charged sediments were identified by characteristic "seismic smearing", which is also a relatively common phenomenon in Hong Kong waters. One mud diapir was identified in the southeastern part of the Pearl River mouth region, located in approximately 180 m of water. The diapir was reported to be about 1 km wide. Li and Jin considered that the following factors contributed to seafloor instabilities in the region :

4.5.1 Quaternary Sea-level Change

Resulting in migration of the coastline and lateral movement of river channels and facies boundaries. Such movements have resulted in vertical and lateral variations in engineering properties.

4.5.2 Seismicity

Considered by the authors to be an important mechanism, triggering slides in seafloor slope deposits and activating seafloor faults.

4.6 Submarine Slope Stability in Hong Kong Waters

The following general conclusions can be reached from examination of Hong Kong's regional setting and depositional environments :

(1) Modern net sedimentation rates in Hong Kong are very low;

(2) The Holocene marine soils of Hong Kong were deposited relatively slowly and are normally consolidated;

(3) The existing seabed topography of Hong Kong probably reflects a state of dynamic equilibrium and, in the absence of hydrodynamic changes, can be expected to be generally stable, although the surface layers of sediment may be highly mobile;

(4) Occasional incursions of sediment from the Pearl River may temporarily disrupt the general stability of the sedimentary regime;

(5) Marine construction works can be expected to have an influence on the stability of the natural seabed;

(6) Exceptional natural events such as severe typhoons, earthquakes or large sediment incursions may affect the natural stability of the seabed topography.

5. NATURAL SLOPES, NORTH LANTAU

5.1 Study Area

The area chosen for study was centred on Chek Lap Kok (see Figure 10), due to the large amount of hydrographic, oceanographic and soil data available for this area. A distinction was made between sites to the east and west of Chek Lap Kok as the oceanographic regimes in these areas differ.

The marine deposits in the Chek Lap Kok area have been extensively investigated and comprise soft marine clays that are occasionally sandy and which contain some shell fragments. Occasional thin beds of loose marine sand are also present. The total thickness of marine deposits varies, ranging from less than one metre in places (generally close inshore) to over 20 m.

The theoretical slope model adopted for this study utilises normalised shear strength (c_u/σ'_{vo}). Premchitt et al (1990), using insitu vane tests, confirmed average normalised shear strength ratios of 0.42 for the soft marine clays at Chek Lap Kok, on the basis of data from 1981 and 1990 site investigation works.

The oceanographic characteristics of the area are described in some detail in Civil Engineering Office (1982). This report arrived at design wave heights and storm surge levels for 10, 20, 50, 100, 500 and 1000 year return periods by calculation, using wind speeds, fetch, refraction and shoaling as input parameters. The design wave height and storm surge levels are extreme (maximum) values. Points on the west, east and north coasts of Chek Lap Kok were considered. The design values derived for the north coast are almost identical to those derived for the west coast. The design values calculated for the east and west coasts have been applied to sites to the east and west of Chek Lap Kok respectively. Design wave heights west of Chek Lap Kok are significantly higher than those east of Chek Lap Kok, whereas storm surge levels in the east are higher than in the west.

5.2 Natural Slopes

Data on natural slopes in the area were obtained from three hydrographic/geophysical surveys performed between 1979 and 1990. Slope gradients, slope heights, mean water depths and marine deposit thicknesses were measured for a total of 46 and 63 slopes east and west of Chek Lap Kok respectively. Water depths, presented on the survey plans referenced to Principal Datum, were corrected to Mean Sea Level by the addition of 1.30 metres.

Natural slope angles were examined for relationship with slope height, mean water depth (below MSL) and marine deposit thickness. The only significant association was that of slope angle against water depth. The apparent relation of slope angle with water depth suggests a governing mechanism dominated by wave forces, which decrease with water depth, and this hypothesis was adopted as the basis of the theoretical model.

5.3 Theoretical Model

It was assumed for this study that the bedforms are determined by extreme events. It was also assumed, for the purposes of the analysis, that the maximum wave height occurs simultaneously with the maximum storm surge. A 1,000 year return period was used to model these extreme events. The calculated 1000-year deep-water wave heights and periods, H_0 and T_0, east and west of Chek Lap Kok are 3.30 m, 6.2 seconds and 3.55 m, 7.5 seconds respectively (CEO, 1981). After allowance for refraction effects the wave heights become 3.23 m and 4.26 m for the eastern and western areas. It can be seen that refraction is concentrating wave energy in the area to the west of Chek Lap Kok. The above data are taken directly from Study Report #3 of Civil Engineering Office (1982).

As the 1000-year waves move into shallow water, shoaling effects will change their height. Note that wave height may increase as the water depth decreases. Study Report #3 corrects the deep-water wave heights to a single appropriate water depth according to the methods of the Shore Protection Manual (US Army Corps of Engineers, 1984). For this report the wave heights have been further corrected in the same manner for various depths, to model the situation of a wave moving into shallow waters. Plots of predicted wave height against water depth are given in Figure 11.

The water depths and wave heights at which the design waves are likely to break have been calculated. Water depths are 4.08 m and 5.43 m, while wave heights are 3.39 m and 4.60 m, east and west of Chek Lap Kok respectively. An average beach slope of 2° was assumed for these calculations. The predicted wave breaking points are shown on Figure 12, together with calculated bottom pressures and wavelengths.

Using Henkel's graphical solution (Henkel, 1970, described in Evans, 1992) for a range of slope angles from 0.1 degrees to 11 degrees, a series of potential failure curves has been calculated relating bottom pressure required for failure to failure depth and water depth (see Figures 13 and 14). The predicted bottom pressures resulting from the design waves have been superimposed to show where failure is possible.

Figure 15 shows the potential failure depths for various slope angles and water depths as extracted from Figures 13 and 14. Examination of Figure 15 shows that there is a theoretical maximum slope gradient associated with each depth of water. The situation in shallow, wave-breaking water is more complex, but slope processes here are expected to be dominated by scour and reworking of soil, and slopes in this zone may be regarded as partially mobile. The water depths referred to in Figures 13 to 15 relate to the storm surge level and not to Mean Sea Level. Civil Engineering Office (1982) estimates the 1000-year storm surge level to be +4.95 mPD and +4.75 mPD for east and west of Chek Lap Kok respectively. These figures equate to 3.65 m and 3.45 m above Mean Sea Level. Figure 16 shows the theoretical maximum slope gradient against water depth, corrected to Mean Sea

Level, superimposed on the observed existing slopes.

The observed gradients of natural submarine slopes in the Chek Lap Kok area nowhere exceed the predicted maximum gradients. The agreement between the predicted and the observed gradients is good, suggesting that the theoretical model used is reasonable. It would appear that long-term natural stable slope angles in relatively shallow water are governed by extreme wave and storm surge levels.

6. DREDGED SLOPES, PLOVER COVE

Ford and Elliot (1965) describe the investigation and design work associated with the construction of Plover Cove Reservoir in the northeast New Territories. As part of this work a test mound was constructed close to the main dam site, with the seabed mud being dredged to different gradients. The performance of these slopes was then monitored.

Plover Cove forms part of a large drowned valley (Tolo Harbour and Tolo Channel) which, even before dam construction, was sheltered from the open sea. The seabed strata typically comprise about 10 m of dark grey marine mud overlying heterogeneous alluvial deposits. The clay content of the muds varies from 47% to 64%. The original seabed level is generally about -5 mPD to -10 mPD. Wave heights are limited by the restricted fetch and may be regarded as being negligible in all but extreme weather.

About 100 boreholes were sunk at the site by shell and auger techniques, with undrained shear strengths measured insitu by field vane testing gear, and in the laboratory by unconfined compression tests and undrained triaxial tests. The undrained shear strength characteristics of the mud were examined in detail by Lumb and Holt (1968), who derived a c_u/σ_{vo}' ratio of 0.396, using average strength at average depth.

Using Equation (1) it can be seen that this material, in the absence of external dynamic forces, should be stable at angles of up to 26 degrees, or 1 in 2. Examination of the as-built profiles of the test cuts (Figure 17) would seem to confirm this theoretical stable slope angle. Significant slope regression was seen to occur at an as-built gradient of 1 in 1.2, with some limited regression at 1 in 1.7. Slopes cut at gradients of 1 in 2 and 1 in 3 appear to be generally stable.

7. DREDGED SLOPES, URMSTON ROAD

As part of the Tin Shui Wai development, fifteen borrow pits for the supply of sand and gravel were dredged in Urmston Road between January 1988 and June 1990 (Figure 18). Eight of these borrow pits were later backfilled with spoil, but seven remained open when a bathymetric survey was carried out between 27 June and 20 July 1990. The borrow pit area had been the subject of a fairly comprehensive site investigation performed in late 1985. Combination of the site investigation data and the bathymetric data has enabled stability analyses to be conducted as part of this study for the borrow pit sideslopes as standing at the time of the bathymetric survey. At the time of the survey the average age of the sideslopes was about 10 months. Analysis of these slopes therefore provides a good example of the stability of dredged slopes in the short to medium term.

Cross-sections were prepared from the available information. Two typical cross-sections are shown in Figure 19. The geology comprises 5 m to 20 m of marine silts and clays overlying sands and gravels that are generally alluvial and which contain some clay bands. The cut slopes therefore comprise an upper portion consisting of the marine silts and clays, with a variable thickness of sand and gravel generally exposed at the base of the slope. Some of the slopes comprise silt and clay for their full height. It can also be seen that the slope gradients increase with depth and that the slopes in the sands and gravels are steeper than those in the silts and clays. Water depths at the slope crests vary from about 6 m to 20 m, while maximum water depth in the base of the pits is about 40 m.

7.1 Geotechnical Characteristics

Bulk densities in the silts and clays ranged from 1.45 Mg/cu m to 1.73 Mg/cu m with an average of 1.60 Mg/cu m. Laboratory measurements of drained friction angles in marine silts and clays at Chek Lap Kok gave values of 28 degrees (Premchitt et al, 1990), and this value was adopted. Field vane shear strength data from the site indicate representative c_u/σ'_{vo} values of 0.26 above a level of 6.5 mPD and 0.48 below 6.5 mPD.

SPT N values from the sands and gravels at the site were corrected for overburden to N_1 values for this study. Friction angle has been estimated from the N_1 values after Smith (1982). Taking points midway between Smith's curves for fine sand and for well-graded sand and gravel, ϕ' values were assessed as 32.5 degrees down to -31 mPD, increasing linearly to 36 degrees at -40 mPD. The SPT N_1 values are very variable, probably as a result of the differing amounts of gravel present. For this reason lower-bound values have been used as these will tend to be most representative of the soil matrix.

7.2 Oceanographic Characteristics

Oceanographic data for the Urmston Road site are limited. However data for a one-year period are available for the Deep Bay borrow area, which is located approximately 5 km to the northeast of the Urmston Road site, and which has similar wave exposure. These data indicate that maximum wave heights of 0.64 m to 0.72 m may be expected on two days per year.

In view of the age of the unfilled pits at Urmston Road it is reasonable to adopt a wave height of 0.7 m, with a calculated wavelength of 40 m (Plate C-2 of the Shore Protection Manual, US Army Corps of Engineers, 1984), using water depths of 6-40 m with a period of five seconds (data from Chek Lap Kok).

Using the standard formula (Equation (3)) the bottom pressures generated in different water depths by the one-year event have been calculated, and range from 2.4 kPa in 6 m of water to 0.03 kPa in 35 m of water.

7.3 Stability

The static (no wave-induced bottom pressure) stability of the slopes at the Urmston

Road site have been examined in both the drained and the undrained condition. Undrained conditions prevail immediately post-dredging and, as the stresses and pore pressures associated with the slope formation dissipate, drained conditions may become predominant.

The undrained static stability of a cohesive submarine slope can be assessed from Equation (1). The theoretical maximum slope angle pertaining to a specific value of c_u/σ'_{vo} can be calculated. The limiting slope angle in the clays is estimated to be 15.7 degrees (1 in 3.6) above 6.5 m below the natural seabed and 36.9 degrees (1 in 1.3) below this depth. The static drained stability of a cohesive submarine slope can be assessed from Equation (2). The limiting slope angle may be calculated, and is seen to be between 27 degrees (1 in 2) and 29 degrees (1 in 1.8).

In the absence of external forces the limiting angle for the sands and gravels will be the friction angle, ϕ', ie: 32.5 degrees (1 in 1.6) to 36 degrees (1 in 1.4).

The worst-case situation with respect to dynamic stability is the minimum water depth, as here the wave-induced bottom pressures will be greatest and the shear strength of the underlying cohesive soils will be least. In the case of Urmston Road the minimum water depth is about 6 m and here the one-year event has been calculated to produce a bottom pressure of 2.4 kPa.

The effect of the bottom pressure is to induce a shear stress in the underlying soils, and this shear stress will reach a maximum of 0.368 p_0 at a depth of 0.159 d/L, where p_0 is the bottom pressure, d is the depth below the mudline and L is the wavelength (Poulos, 1988). For the worst-case situation above, it can be shown that, with p_o = 2.4 kPa and L = 40 m, a maximum shear stress of 0.88 kPa is induced at a depth of 6.36 m. The estimated shear strength at a depth of 6.36 m below natural seabed is at least 10 kPa, hence shear failure under the wave load is unlikely even under the worst-case conditions. It is therefore concluded that the estimated 1-year wave event will have little effect on the stability of the silts and clays. The induced bottom pressures at the depths at which the sands and gravels are found are negligible and it must be concluded that the one-year event will have no effect on the stability of the soils at this site.

Data on actual slope angles, soil conditions, water depths and depths below natural seabed were obtained from the cross-sections and are shown in Figure 20 compared with theoretical maximum slope angles. The data for silts and clays indicate that the measured angles are less than predicted maximum slope angles, suggesting that the predictive model is reasonable. The fact that no measured slope angles exceed the theoretical drained maximum indicates that equilibrium under drained conditions may have occurred. The data for the sands and gravels are less comprehensive than is the case for the silts and clays but the measured angles are also less than the predicted maximum angles.

8. CONCLUSIONS

The existing natural seabed topography of Hong Kong may be regarded as generally stable and as being in a state of dynamic equilibrium with the generally mild erosional/depositional environment. Civil engineering works which change the natural topography and/or the hydrodynamic regime can be expected to have a greater effect on submarine slope stability than natural events. Extreme natural events may, however, exacerbate any inherent instability caused by engineering works. The seabed of the western Pearl River estuary around Macau is, by contrast, a highly dynamic and potentially unstable area.

Study of natural slopes off North Lantau confirms that the existing seabed is in equilibrium. Seabed topography in shallow water in this area has been shown to be related to long-term (1,000 year) wave height and water level conditions.

Comparison of observed and predicted maximum gradients in dredged borrow pits in Urmston Road, and in test cuts at Plover Cove, suggests that theoretical methods can be used to give reasonable predictions of short to medium term stable dredged slope angles. These angles will vary with soil properties and site characteristics, ie : water depth and wave regime.

9. REFERENCES

Almagor, G., Bennet, R.H., Lambert, D.N., Forde, E.B. & Shepard, L.S. (1984). Analysis of slope stability, Wilmington to Lindenkohl canyons, US Mid-Atlantic margin. In Seabed Mechanics, edited by B. Denness, pp 77-86, Graham and Trotman, London.

Bea, R.G., Wright, S.G., Sircar, P. & Niedoroda, A.W. (1983). Wave-induced slides in South Pass Block 70, Mississippi Delta. Journal of Geotechnical Engineering, ASCE, vol. 109(4), pp 619-644.

Bishop, A.W. (1955). The use of the slip circle in the stability analysis of slopes. Geotechnique, vol. 23(3), pp 7-17.

Bolton, M.D. (1986). Strength and dilatancy of sands. Géotechnique, vol. 36(1), pp 65-78.

Booth, J.S. & Garrison, L.E. (1978). A geologic and geotechnical analysis of the upper continental slope adjacent to the Mississippi Delta. Proceedings of the 10th Annual Offshore Technology Conference, Houston, Texas, pp 1019-1028.

Booth, J.S., Silva, A.J. & Jordan, S.A (1984). Slope stability analysis and creep susceptibility of quaternary sediments on the northeastern United States continental slope. In Seabed Mechanics, edited by B. Denness, pp 65-75, Graham and Trotman, London.

Chalmers, M.L. (1984). Preliminary assessment of sedimentation in Victoria Harbour, Hong Kong. In Geology of Superficial Deposits in Hong Kong, Geological Society of Hong Kong Bulletin No. 1, pp 117-129.

Civil Engineering Office, (1982). Replacement Airport at Chek Lap Kok, Civil Engineering Design Studies, Study Report #3. Oceanographic Investigations, Final Report. Engineering Development Department.

Coleman, J.M. & Garrison, L.E. (1977). Geological aspects of marine slope stability, Northwestern Gulf of Mexico. Marine Geotechnology, vol. 2, pp 9-44.

Coleman, J.M. & Prior D.B. (1978). Submarine landslides in the Mississippi River Delta. Proceedings of the 10th Annual Offshore Technology Conference, Houston, Texas, pp 1067-1074.

De Josselin de Jong, G. (1976). Rowe's stress-dilatancy relation based on friction. Géotechnique, vol. 26(3), pp 527- 534.

Denlinger, R.P. & Iverson, R.M. (1990). Limiting equilibrium and liquefaction potential in infinite submarine slopes. Marine Geotechnology, vol. 9, pp 299-312

Edgars and Karlsrud (1982). Soil flows generated by submarine slides - case studies and consequences. Proceedings of the 3rd BOSS Conference, Cambridge, Massachusetts, vol. 2, pp 425-437.

Evans, C.D.R. (1988). Seismo-stratigraphy of early Holocene sand banks. Marine Sand and Gravel Resources of Hong Kong, Geological Society of Hong Kong, pp 45-52.

Evans, N.C. (1992). Geotechnical Aspects of Mud Dredging and Dumping. Special Project Report SP 13/92, Geotechnical Engineering Office, Civil Engineering Department, Hong Kong Government, 50 p.

Evans, N.C. & Premchitt, J. (1991). Submarine Slope Stability at South Tsing Yi Marine Borrow Area. Technical Note TN 9/91. Geotechnical Engineering Office, Civil Engineering Department, Hong Kong Government, 33p.

Ford, S.E.H. & Elliott, S.G. (1965). Investigation and design of the Plover Cove Water Scheme. Proceedings of the Institution of Civil Engineers, vol. 32, pp 255-293.

Gibson, R.E. (1958). The progress of consolidation in a clay layer increasing in thickness with time. Géotechnique, vol. 8, pp 171-182.

Henkel, D.J. (1970). The role of waves in causing submarine landslides. Géotechnique, vol. 20(1), pp 75-80.

Hyde, A.F.L. & Ward, S.J. (1985). A pore pressure and stability model for a silty clay under repeated loading. Géotechnique, vol. 35, no. 2, pp 113-125.

Hydraulics Research and Water Research Centre (1983). Harbour Reclamation and Urban in Hong Kong; Mathematical Studies of Proposed Schemes on Tidal Flow and Water Quality, Report EX 1081 (unpublished), 73p.

Isihara, K. (1977). Pore water pressure response and liquefaction of sand deposits during earthquakes. Proceedings of DM SR77, Karlsruhe, vol. 2, pp 161-193.

Isihara, K. & Yamazaki, A. (1984). Wave-induced liquefaction in seabed deposits of sand. Seabed Mechanics, edited by B. Denness, pp 139-148. London: Graham and Trotman.

Iwasaki, T., Arakawa, T. & Tokida, K.-I. (1984). Simplified procedures for assessing soil liquefaction during earthquakes. Soil Dynamics and Earthquake Engineering, vol. 3(1), pp 49-58.

Janbu, N. (1973). Slope stability computations. Embankment-Dam Engineering, edited by R.C. Hirschfield & S.J. Poulos, pp 43-86. New York: Wiley.

Kirby, R. (1991). Draft Report on Sediment Transport in Hong Kong and Adjacent Waters and the Implications for Mud Dumping, 64 p.

Lambe, T.W. & Whitman, R.V. (1979). Soil Mechanics, SI Version. John Wiley & Sons Inc., 553p.

Lewis, K.B. (1971). Slumping on a continental slope inclined at 1-4°. Sedimentology, vol. 16, pp 97-110.

Li, C.-C. & Wang, W.-J. (1985). Sedimentation on the Zhujiang River mouth region. In: Modern Sedimentation in Coastal and Nearshore Zones of China, M.-E. Ren, editor, China Ocean Press, Beijing, China, pp 230-251.

Li, T. & Jin, B. (1989). Seismic facies analysis of the seafloor instabilities in the Pearl River Mouth Region. Marine Geotechnology, vol. 8, pp 19-31.

Lo, K.Y. & Lee, C.F. (1973). Stress analysis and slope stability in strain-softening materials. Géotechnique, vol. 23, no. 1, pp 1-11.

Lumb, P. & Holt, J.K. (1968). The undrained shear strength of a soft marine clay from Hong Kong. Géotechnique, vol. 8, pp 25-36.

Lumb, P. (1977). The marine soils of Hong Kong and Macau. Proceedings of the International Symposium on Soft Clay, Bangkok, Thailand, pp 45-58.

Lunne, T. & Christoffersen, H.P. (1983). Interpretation of cone penetrometer data for offshore sands. Proceedings of the 15th Offshore Technology Conference, Houston, vol. 1, pp 181-192.

Meijer, K.L. & van Os, A.G. (1976). Pore pressures near moving underwater slope. Journal of the Geotechnical Engineering Division, ASCE, vol. 102, no. GT4, pp 361-372.

Moore, D.G. (1978). Submarine slides. Rockslides and Avalanches, vol. 1: Natural Phenomena, edited by B. Voigt, pp 563-604. Amsterdam: Elsevier.

Morgenstern, N.R. (1967). Submarine slumping and the initiation of turbidity currents. Marine Geotechnique, edited by A.F. Richards, pp 189-220. Urbana: University of Illinois Press.

Morin, P. & Pereira, C.P.G. (1987). Sedimentology, geotechnical properties and stability of the surficial sediments on the continental slope, southwestern Flemish Pass. Marine Geotechnology, vol. 7(4), pp 289-316.

Nataraja, M.S. & Gill, H.S. (1983). Ocean wave-induced liquefaction analysis. Journal of Geotechnical Engineering, ASCE, vol. 109(4), pp 573-590.

Poulos, H.G. (1988). Marine Geotechnics. London: Unwin Hyman, 473 p.

Premchitt, J., To, P.W.T. & Lam, T.S.K. (1990). New Airport at Chek Lap Kok, Geotechnical Investigation (1990), Volume I, Geotechnical Assessment. GCO, Civil Engineering Services Department, Hong Kong. Advisory Report No ADR 13/90, 124p.

Prior, D.B. & Coleman, J.M. (1978). Disintegrating retrogressive landslides on very low-angle subaqueous slopes, Mississippi Delta. Marine Geotechnology, vol. 3(1), pp 37-60.

Prior, D.B. & Suhayda, J.N. (1979). Application of the infinite slope stability analysis to subaqueous sediment instability, Mississippi Delta. Engineering Geology, vol. 14, pp 1-10.

Pun, W.K. (1992). Earthquake Resistance of Buildings and Marine Reclamation Fills in Hong Kong, GEO Report No. 16, Geotechnical Engineering Office, Hong Kong Government, 55p.

Robertson, P.K. & Campanella, R.G. (1985). Liquefaction potential of sands using the CPT. Journal of the Geotechnical Engineering Division, ASCE, vol. 111(3), pp 384-403.

Rowe, P.W. (1962). The stress-dilatancy relation for static equilibrium of an assembly of particles in contact. Proceedings of the Royal Society, vol. 269 A, pp 500-527.

Rowe, P.W. (1969). The relation between the shear strength of sands in triaxial compression, plane strain and direct shear. Géotechnique, vol. 19(1), pp 75-86.

Sangrey, D.A., Castro, G., Poulos, S.J. & France, J.W. (1978). Cyclic loading of sands, silts and clays. Proceedings of the ASCE Special Conference on Earthquake Engineering and Soil Dynamics, Pasadena, vol. 2, pp 836-851.

Science Applications International Corporation (1994). REMOTS Survey of Soft-Bottom Environments in Coastal Waters of Hong Kong, October 5-13 1993, 34p.

Seed, H.B. & Idriss, I.M. (1971). Simplified procedure for evaluating soil liquefaction potential. Journal of the Soil Mechanics and Foundation Engineering Division, ASCE, vol. 97(SM9), pp 1249-1273.

Seed, H.B., Idriss, I.M. & Arango, I. (1983). Evaluation of liquefaction potential using field performance data. Journal of Geotechnical Engineering, vol. 109(3), pp 458-482.

Seed, H.B., Tokimatsu, K., Harder, L.F. & Chung, R.M. (1984). The influence of SPT procedures in soil liquefaction resistance evaluations. Report No. UCB/EERC-84/15, Earthquake Engineering Research Centre, Berkely, California.

Schmertmann, J.H. (1975). Measurement of insitu shear strength. Special Conference on Insitu Measurement of Soil Properties, ASCE, Raleigh, NC, vol. 2, pp57-138.

Singh, A. & Mitchell, J.K. (1968). General stress-strain-time function for soils. Journal of the Soil Mechanics and Foundation Engineering Division, ASCE, vol. 94(SM1), pp 21-46.

Smith, G.N. (1982). Elements of Soil Mechanics for Civil and Mining Engineers (Fifth Edition). Granada Publishing Ltd., 493 p.

Strange, P.J. & Shaw, R. (1986). Geology of Hong Kong Island and Kowloon, Geological Survey Memoir No. 2, Geotechnical Control Office, Civil Engineering Services Department, Hong Kong Government.

US Army Corps Of Engineers (1984). Shore Protection Manual, Vols. I and II. Coastal Engineering Research Center, Dept. of the Army. Waterways Experimental Station, Vicksburg, Mississippi.

Vallejo, L.E. (1981). Stability analysis of mudflows on natural slopes. Proceedings of the Tenth International Conference on Soil Mechanics and Foundation Engineering, Stockholm, Sweden, pp 541-544.

Van Leussen, W. & Nieuwenhuis, J.D. (1984). Soil mechanics aspects of dredging. Géotechnique, vol. 34(3), pp 359-381.

Watkins, D.J. & Kraft, L.M. (1976). Stability of the continental shelf and slope off Louisiana and Texas: geotechnical aspects. Beyond the Shelf Break, American Association of Petroleum Geologists Memoir, pp B1-B33.

Yim, W. W.-S. (1983). Evidence for Quaternary environmental changes from sea-floor sediments in Hong Kong. Preprint, Palaeoenvironment Conference of East Asia from the Mid-Tertiary, Centre of Asian Studies, University of Hong Kong, 17 pp.

LIST OF FIGURES

Figure No.		Page No.
1	Surface Failure Types in Weak Sediments - I	32
2	Surface Failure Types in Weak Sediments - II	33
3	Structural Features Associated with Seafloor Instability - I	34
4	Structural Features Associated with Seafloor Instability - II	35
5	Structural Features Associated with Seafloor Instability - III	36
6	Relation Between Undrained Shear Strength and Plasticity Index for Normally Consolidated Sediment	37
7	Mudflow Geometry Used for Stability Analysis	38
8	The Run-out Distance of Submarine Slides	39
9	Sedimentary Environments in Hong Kong and Adjacent Waters	40
10	North Lantau and Chek Lap Kok	41
11	North Lantau, Predicted Inshore Wave Heights	42
12	North Lantau, Predicted Wavelengths and Bottom Pressures	43
13	North Lantau, Predicted Depth of Failure for 0.1° to 3° Slope	44
14	North Lantau, Predicted Depth of Failure for 5° to 11° Slopes	45
15	North Lantau, Potential Failure under 1,000-year Wave and Storm Surge Conditions	46
16	North Lantau, Theoretical and Existing Slope Angles	47
17	Performance of Slopes Dredged in Seabed Mud, Plover Cove Reservoir	48
18	Location Plan, Urmston Road Borrow Pits	49
19	Urmston Road Borrow Pits, Cross-sections C-C' and D-D'	50
20	Urmston Road Borrow Pits, Theoretical and Measured Slope Angles	51

Peripheral rotational slump

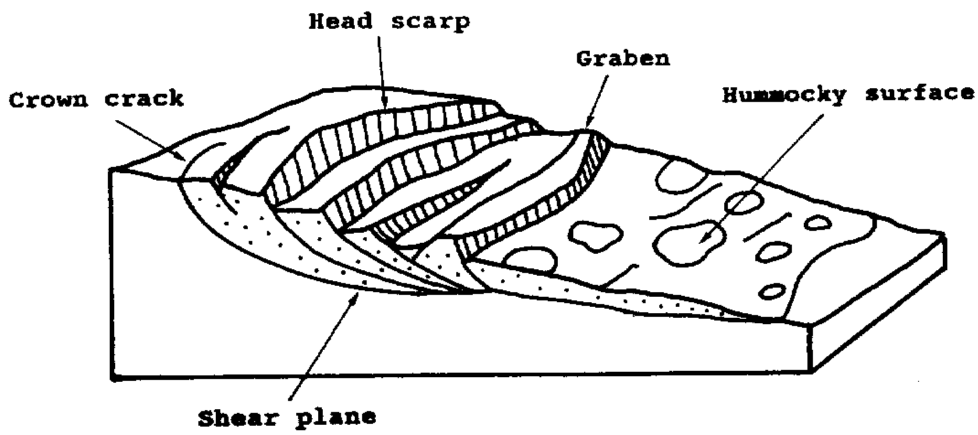

Collapse depression

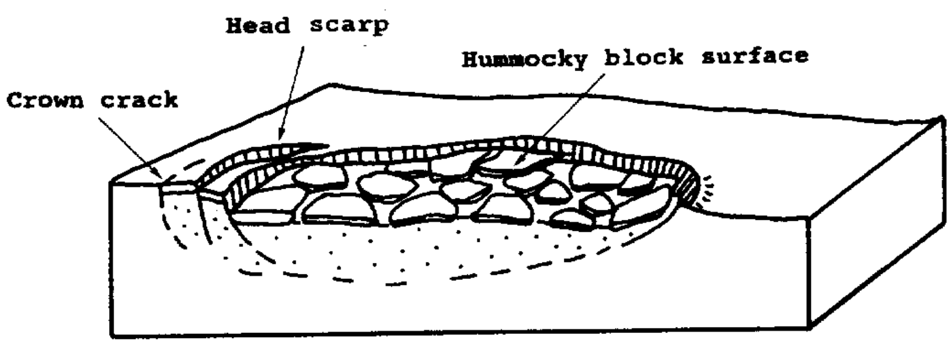

Note: After Coleman and Prior (1978)

Figure 1 - Surface Failure Types in Weak Sediments - I

Bottleneck slide

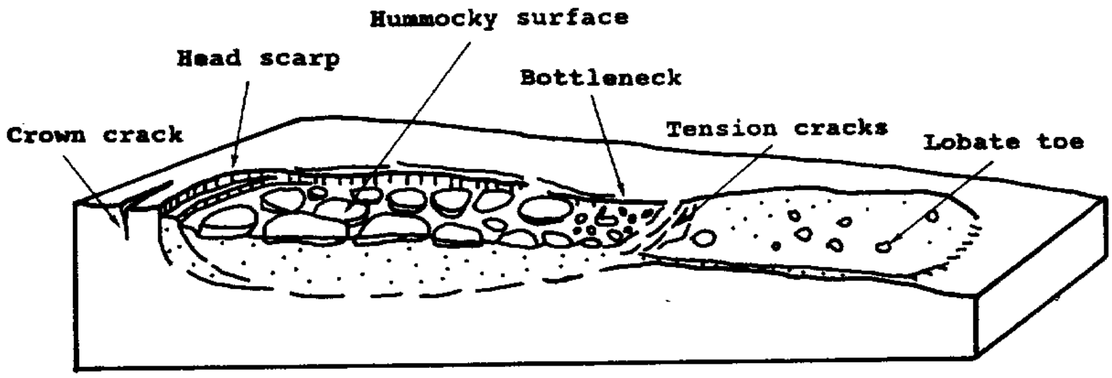

Elongate retrogressive slide

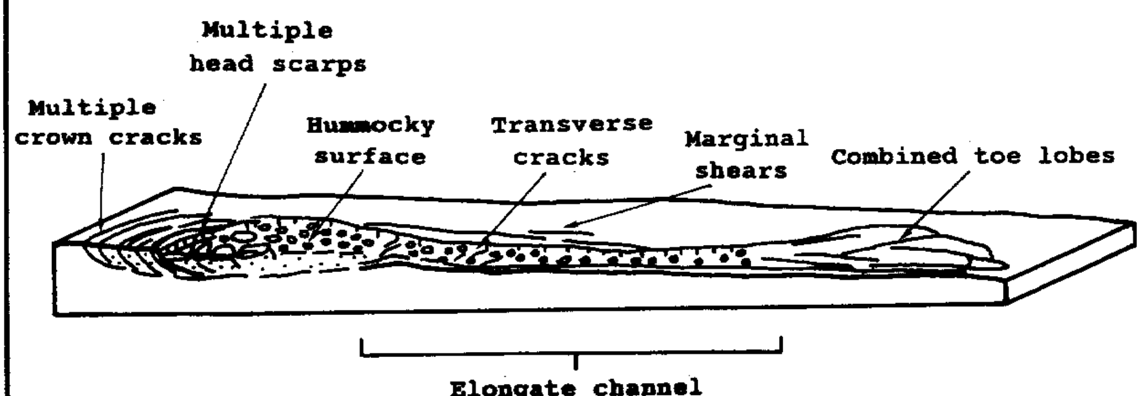

Note: **After Coleman and Prior (1978)**

Figure 2 - Surface Failure Types in Weak Sediments - II

(a) Peripheral Slumps

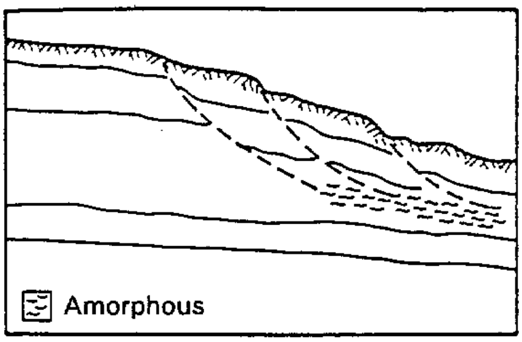

Faulting generally restricted to upper 15m of sediment, and usually parallel or subparallel to bathymetric contours.

(b) Shallow Graben Faults

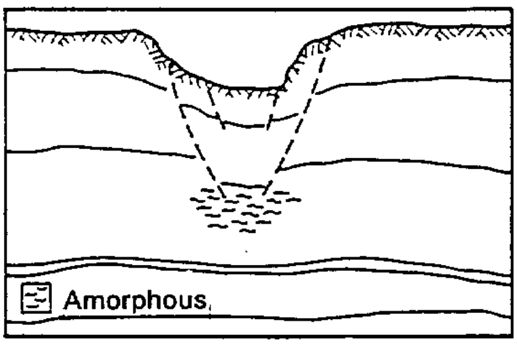

Oriented almost at right angles to the general bathymetry.Often with smooth, flat-bottomed floors.Fault planes generally terminate less than 30m below mudline.

(c) Surface Mudflow

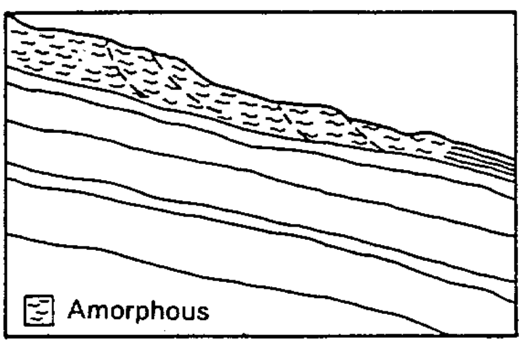

Generally irregular topography.
May extend to depths of 30m.

(d) Growth Fault (Shelf Edge)

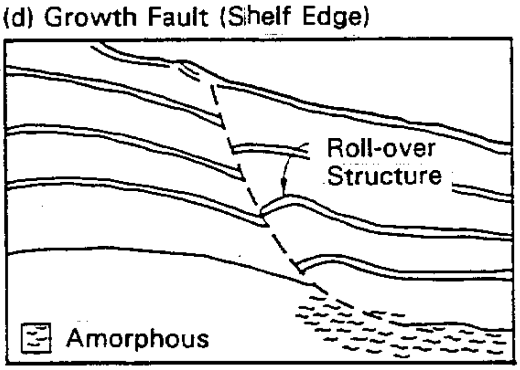

Occur primarily on the upper continental slope. Progressive offset with depth, indicating continuing fault movement during deposition. Fault plane can extend to more than 150m.

NOTE : After Watkins and Kraft (1976) and Poulos (1988)

Figure 3 - Structural Features Associated with Seafloor Instability - I

(a) Convex Fault (Subsurface)

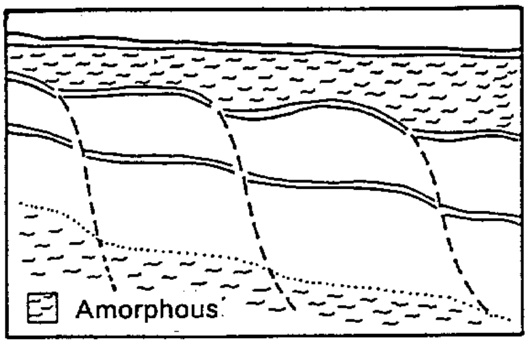

Generally occur in groups.Can extend to over 90m.The fault extremities, both shallow and deep, often terminate in seismically amorphous layers characteristic of disturbance or high gas contents.

(b) Convex Fault (Surface & Subsurface)

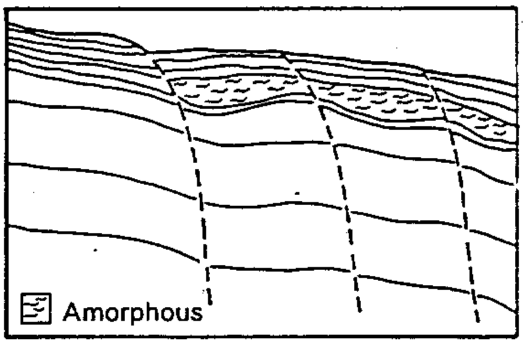

Extend to the surface and may terminate in a scarp of considerable height.

(c) Concave/Convex Fault

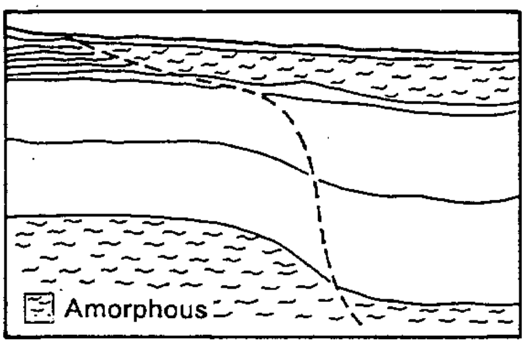

Fault plane is generally not distinct close to the surface.

(d) Complex Shelf Edge Graben Faults

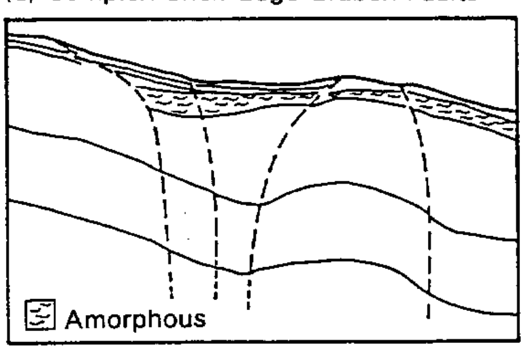

Found at the continental shelf edge, associated with large-scale structural adjustments.The major faults may have seafloor offsets and may penetrate to over 150m.

NOTE : After Watkins and Kraft (1976) and Poulos (1988)

Figure 4 - Structural Features Associated with Seafloor Instability - II

(a) Shelf Edge Slump & Diapiric Intrusion

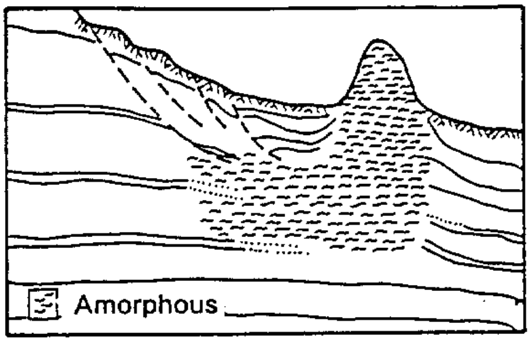

Diapiric intrusions will often form at the base or seaward termination of a slump.

(b) Linear Fault

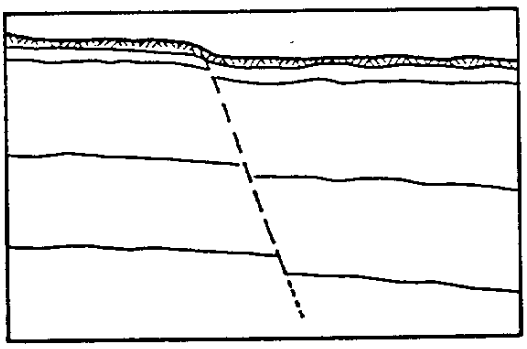

Very simple and well defined.Often penetrate more than 150m.Small surface scarp.Offset usually increases with penetration.

(c) Deep-Seated Faults

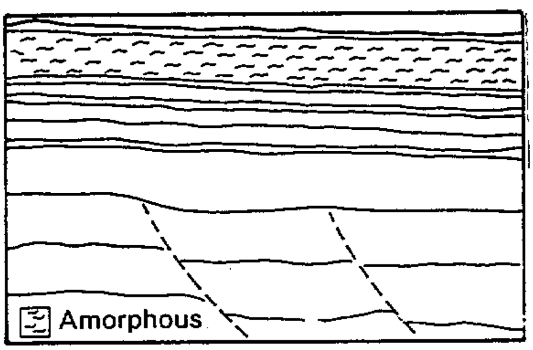

Often occur in groups.Linear to concave upwards, and do not normally cut the near -surface sediments.

(d) Monoclinal Fold

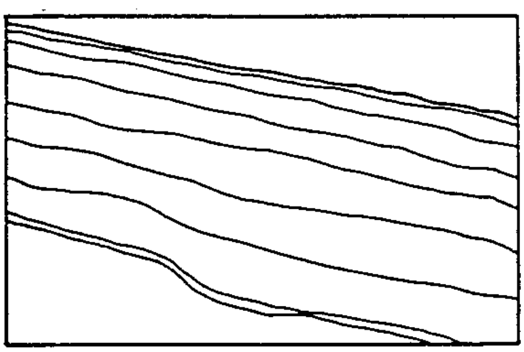

No distinguishable fault plane.
Watkins and Kraft (1976) describe their origin as "somewhat problematical".

NOTE : After Watkins and Kraft (1976) and Poulos (1988)

Figure 5 - Structural Features Associated with Seafloor Instability - III

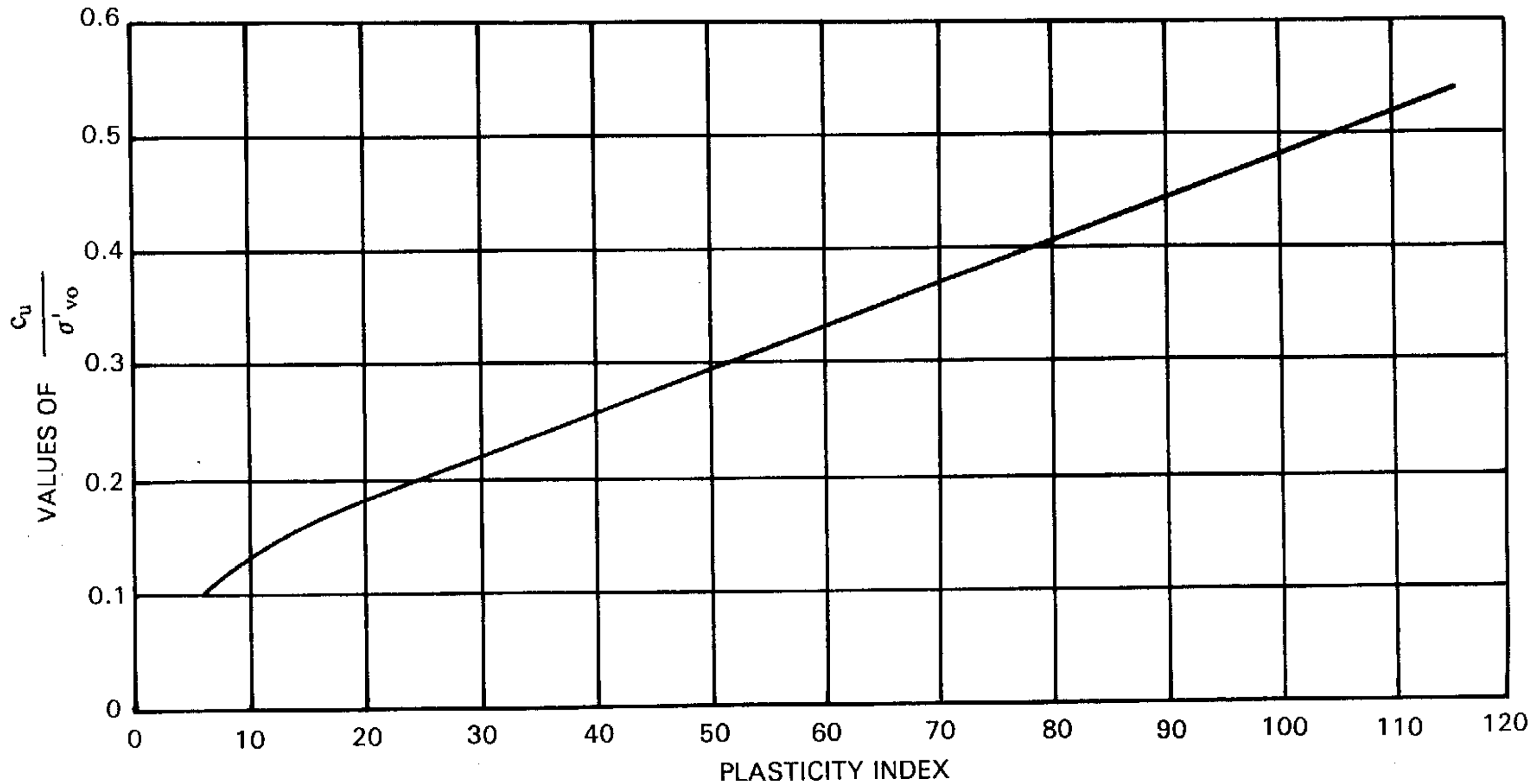

NOTE : After Morgenstern (1967)

Figure 6 - Relation Between Undrained Shear Strength and Plasticity Index for Normally Consolidated Sediment

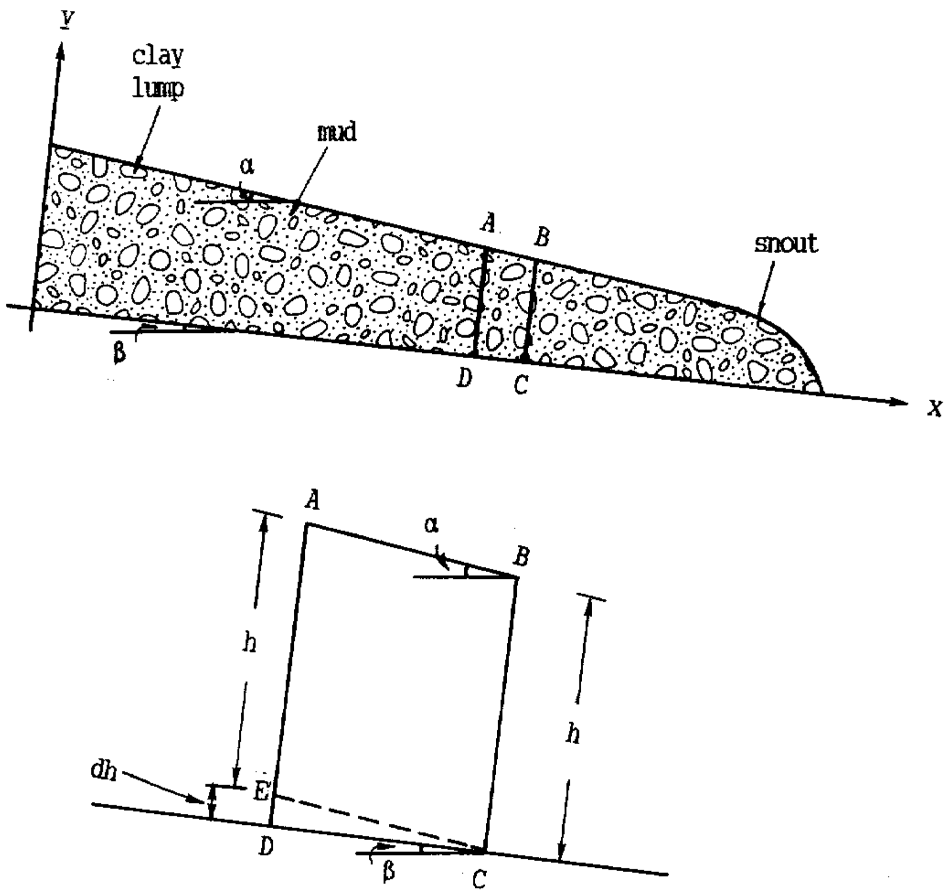

DC = dx

∡ ECD = α − β

Note : After Vallejo (1981)

Figure 7 - Mudflow Geometry Used for Stability Analysis

Definition of Slide Parameters

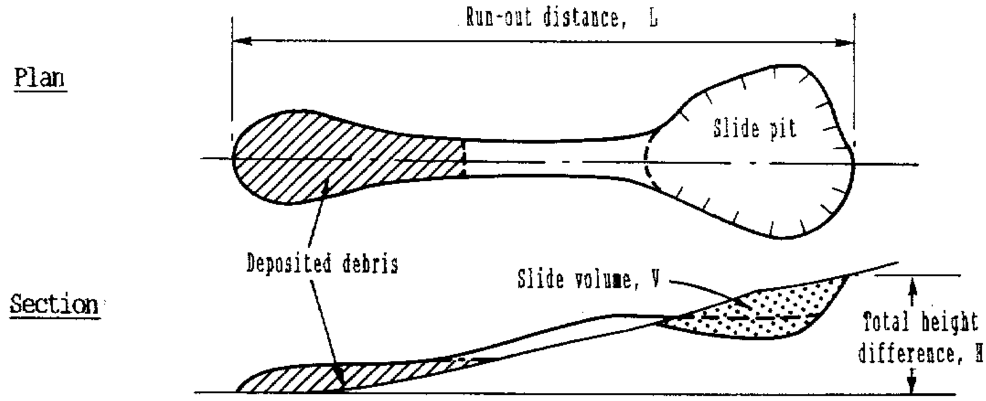

Relative Run-out Distance (L/H) against Slide Volume (V)

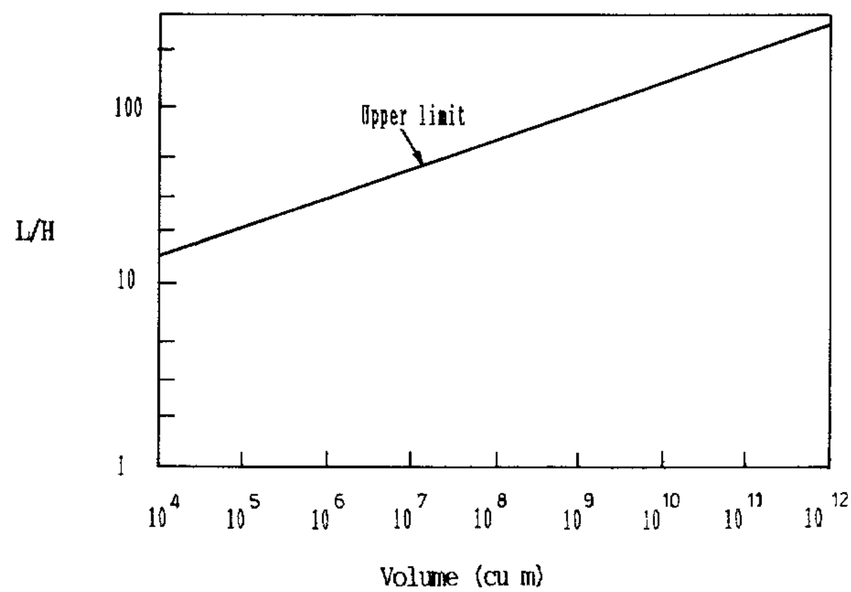

Note : After Edgers and Karlsrud (1982)

Figure 8 - The Run-out Distance of Submarine Slides

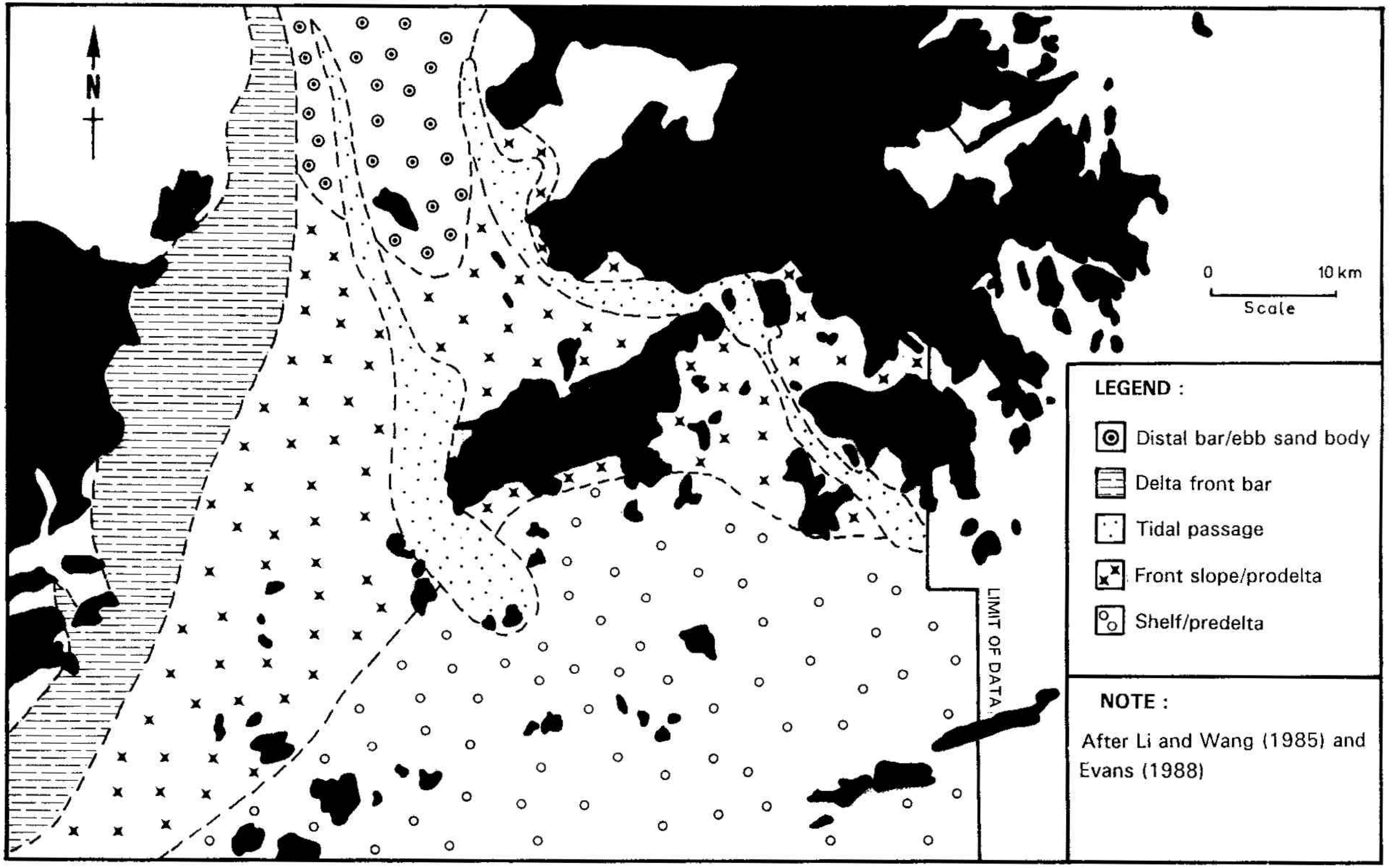

Figure 9 - Sedimentary Environments in Hong Kong and Adjacent Waters

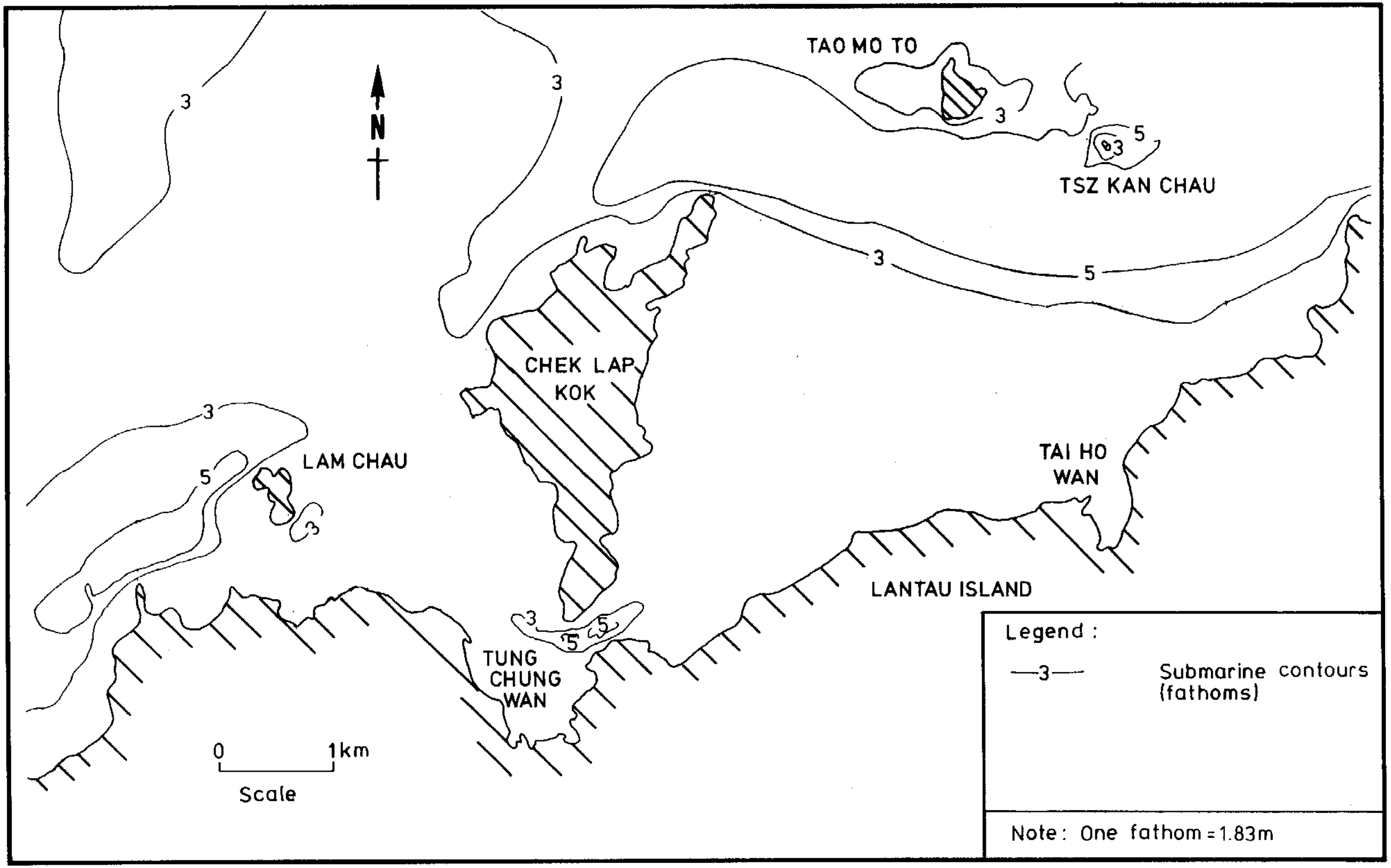

Figure 10 - North Lantau and Chek Lap Kok

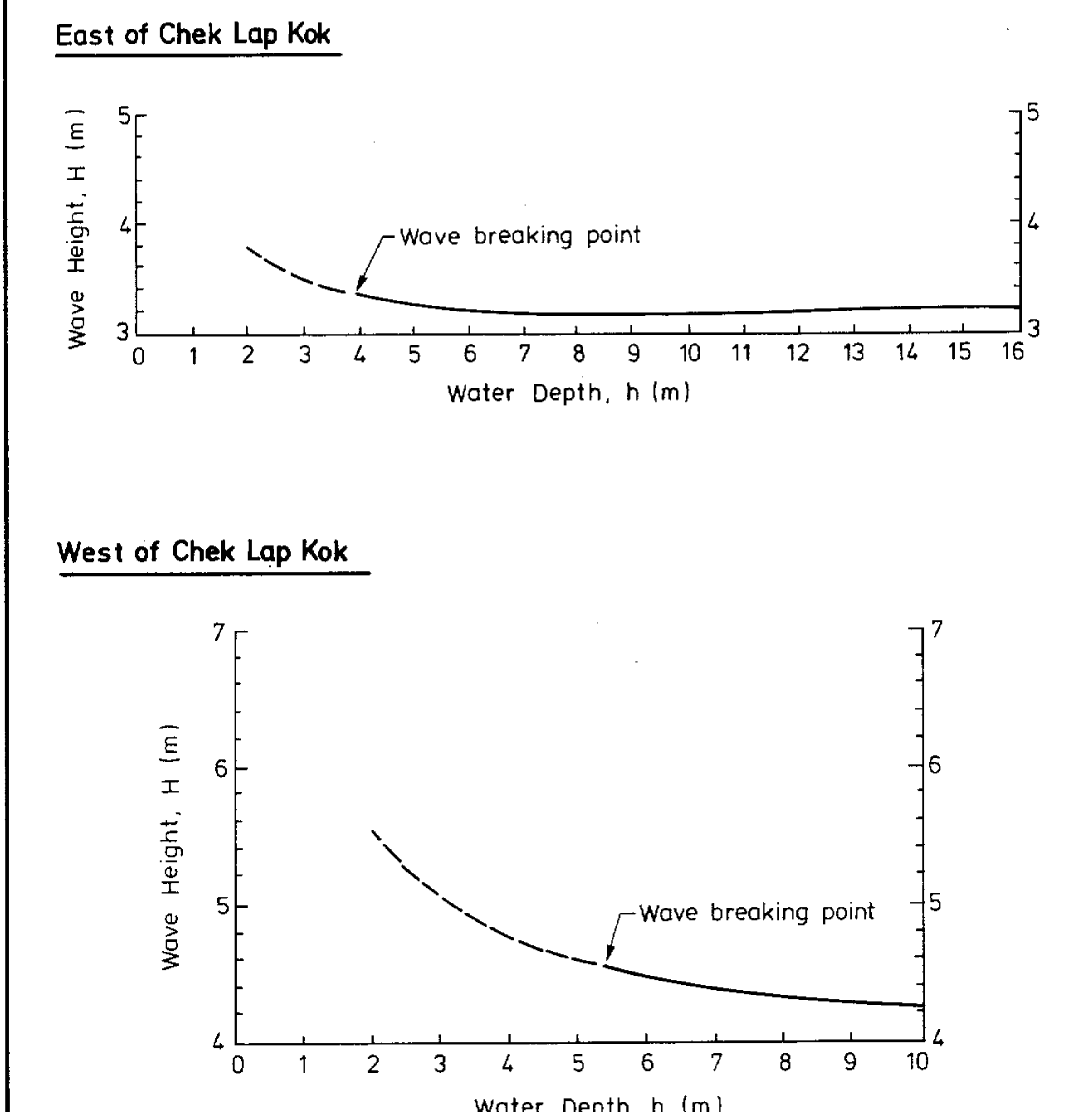

Legend:

———— Wave height corrected for shoaling water

– – – – Theoretical wave height not reached due to breaking of wave

Note : Calculations in accordance with Shore Protection Manual (1984).

Figure 11 - North Lantau, Predicted Inshore Wave Heights

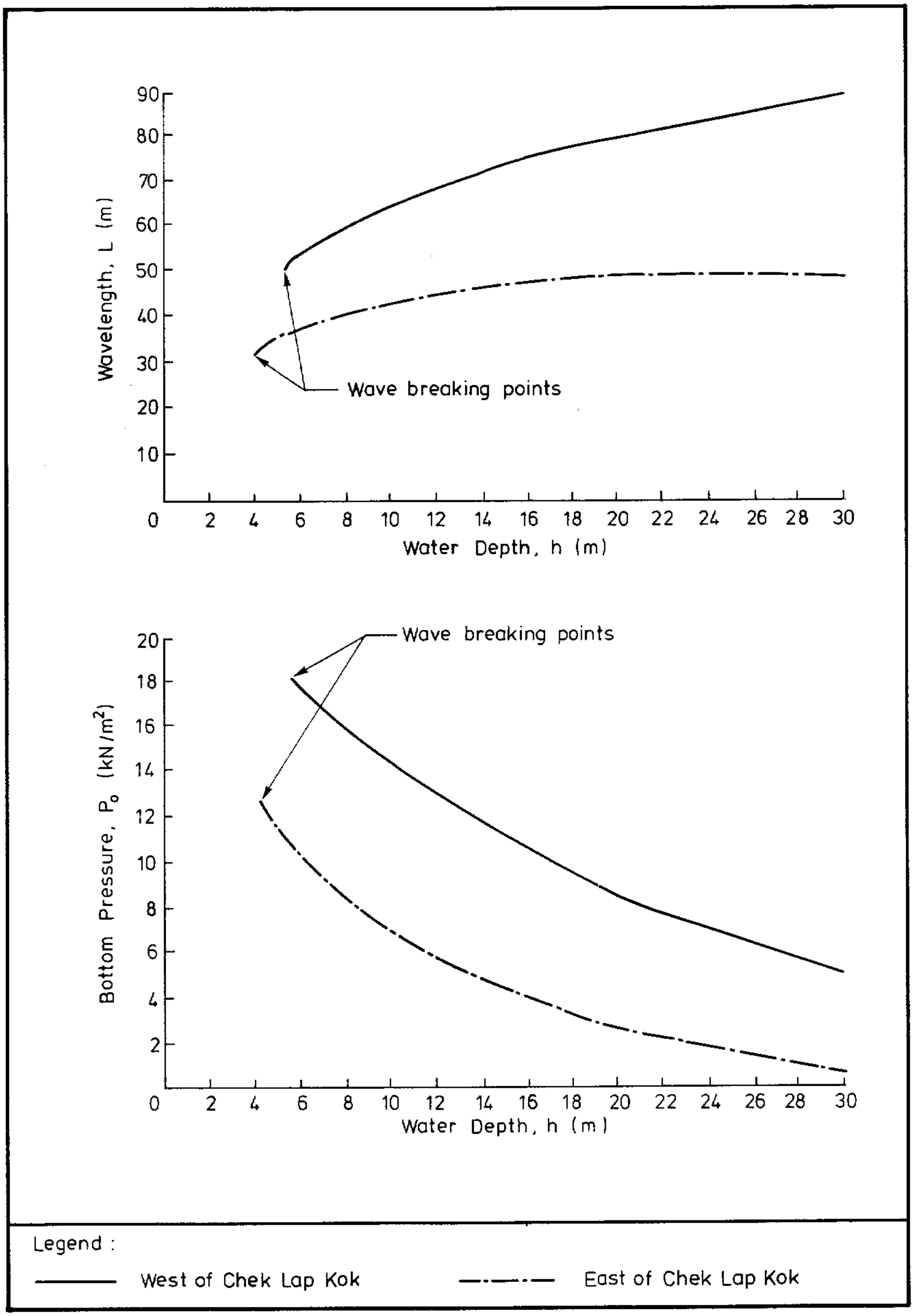

Figure 12 - North Lantau, Predicted Wavelengths and Bottom Pressures

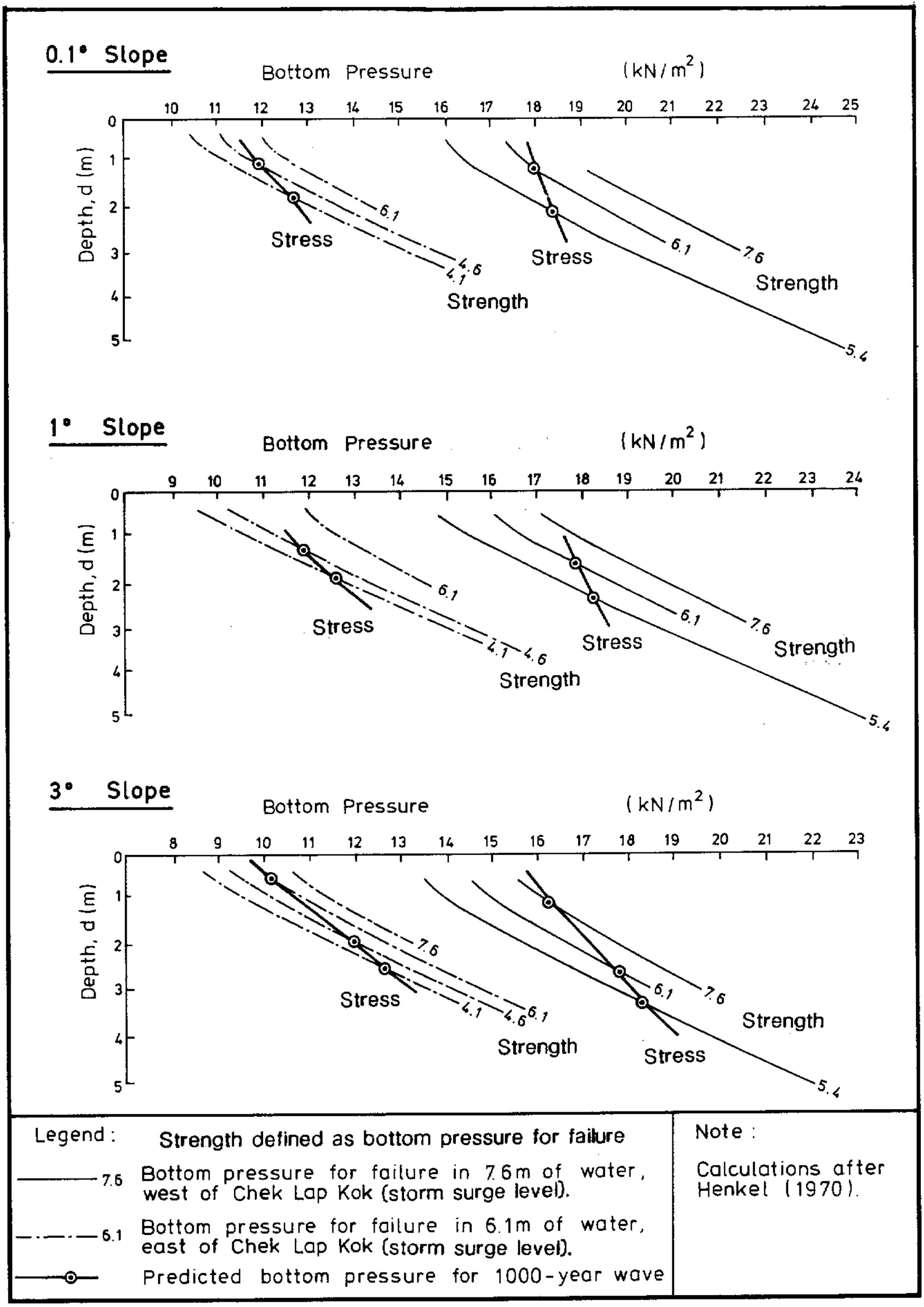

Figure 13 - North Lantau, Predicted Depth of Failure for 0.1° to 3° Slopes

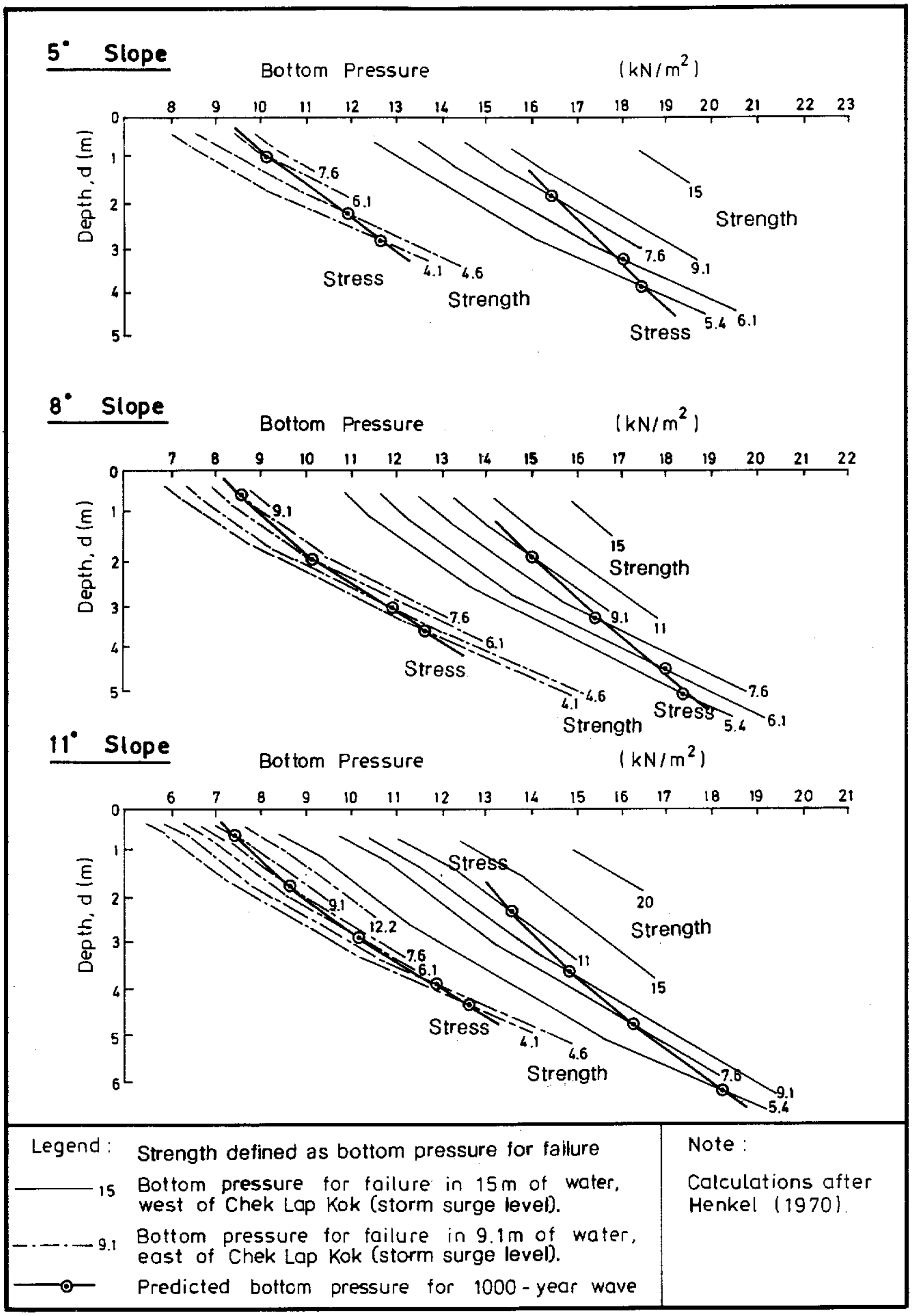

Figure 14 - North Lantau, Predicted Depth of Failure for 5° to 11° Slopes

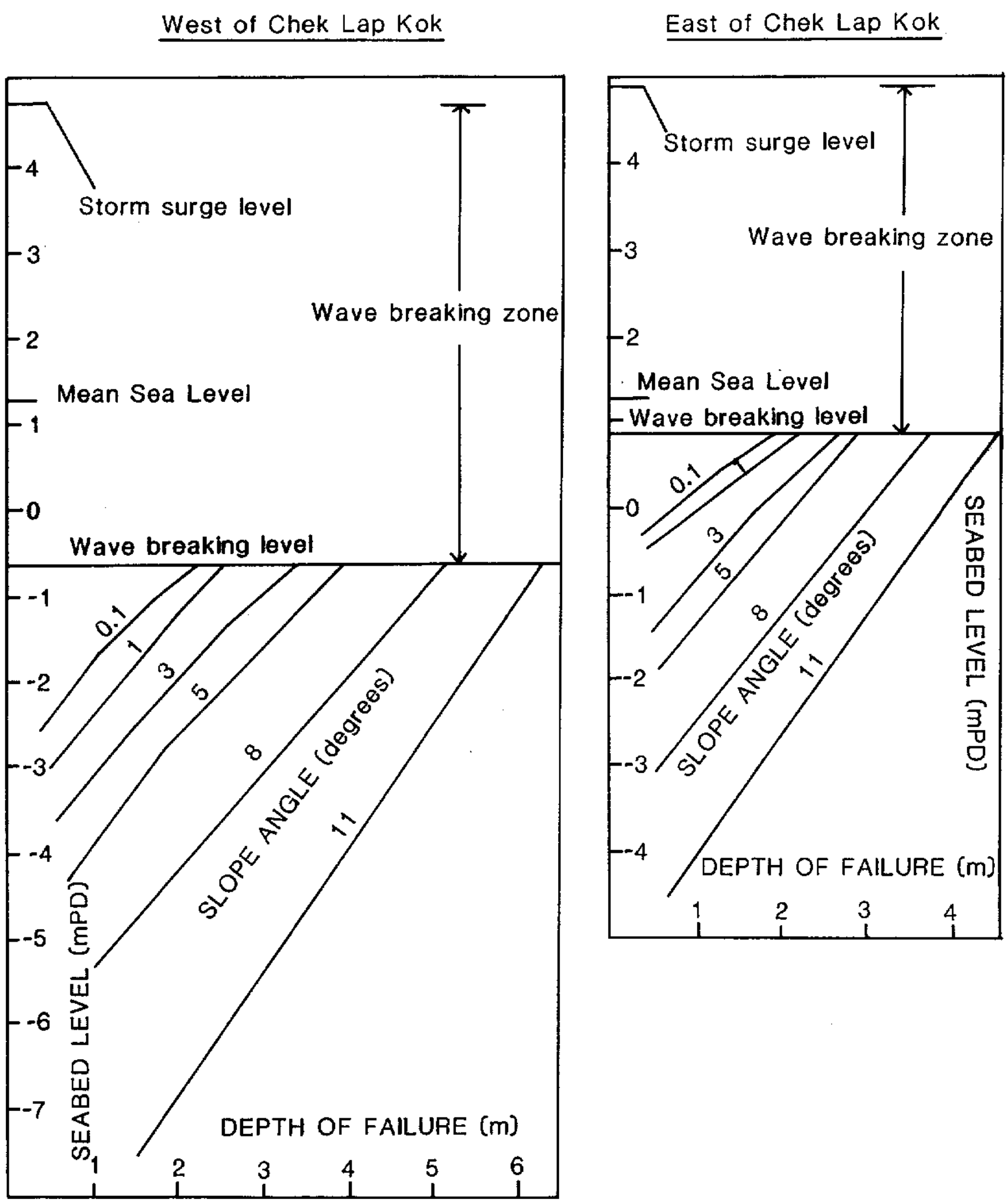

Note: Slope processes in the wave breaking zone are expected to be dominated by scour and re-working.

Figure 15 - North Lantau, Potential Failure under 1,000-year Wave and Storm Surge Conditions

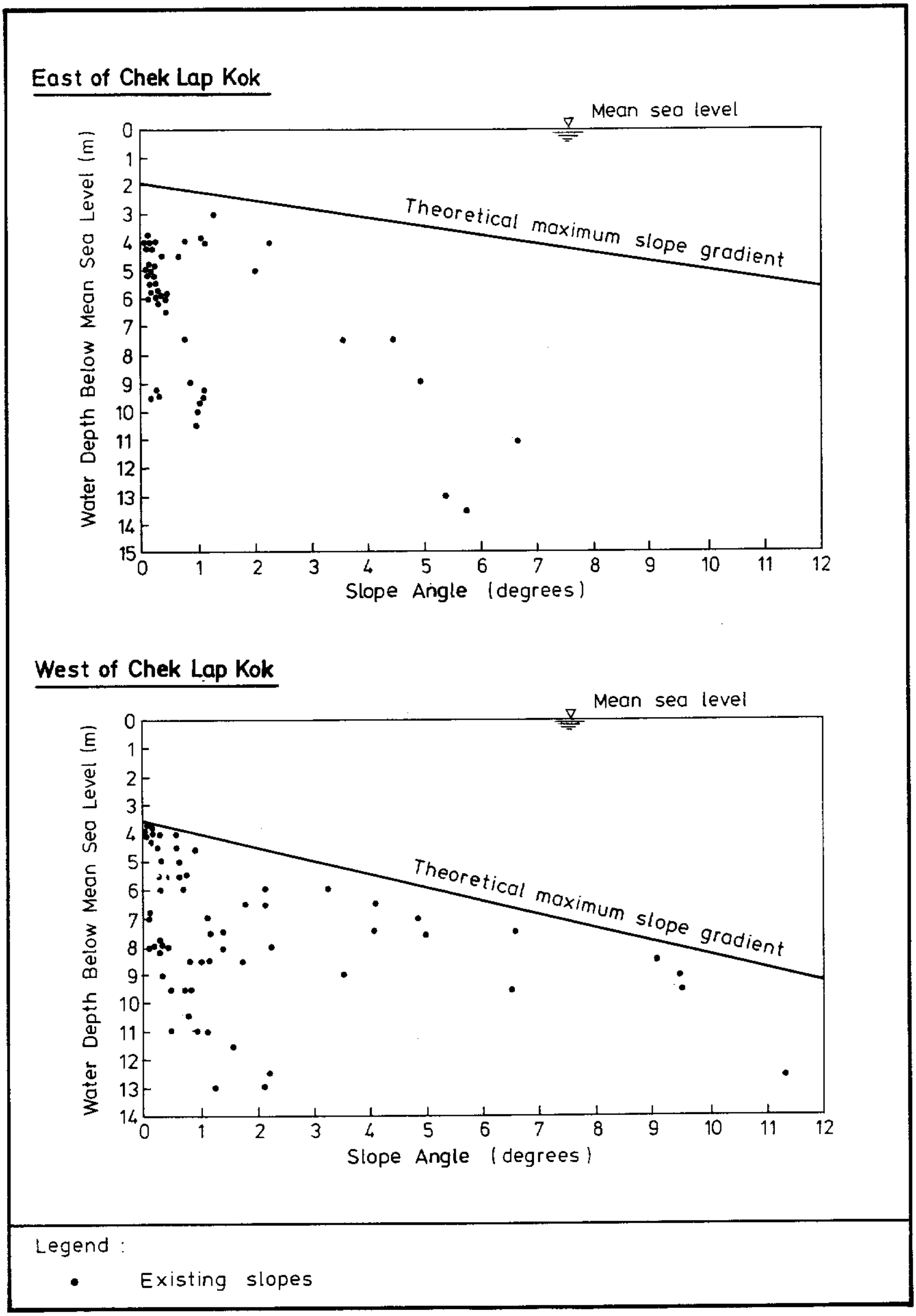

Figure 16 - North Lantau, Theoretical and Existing Slope Angles

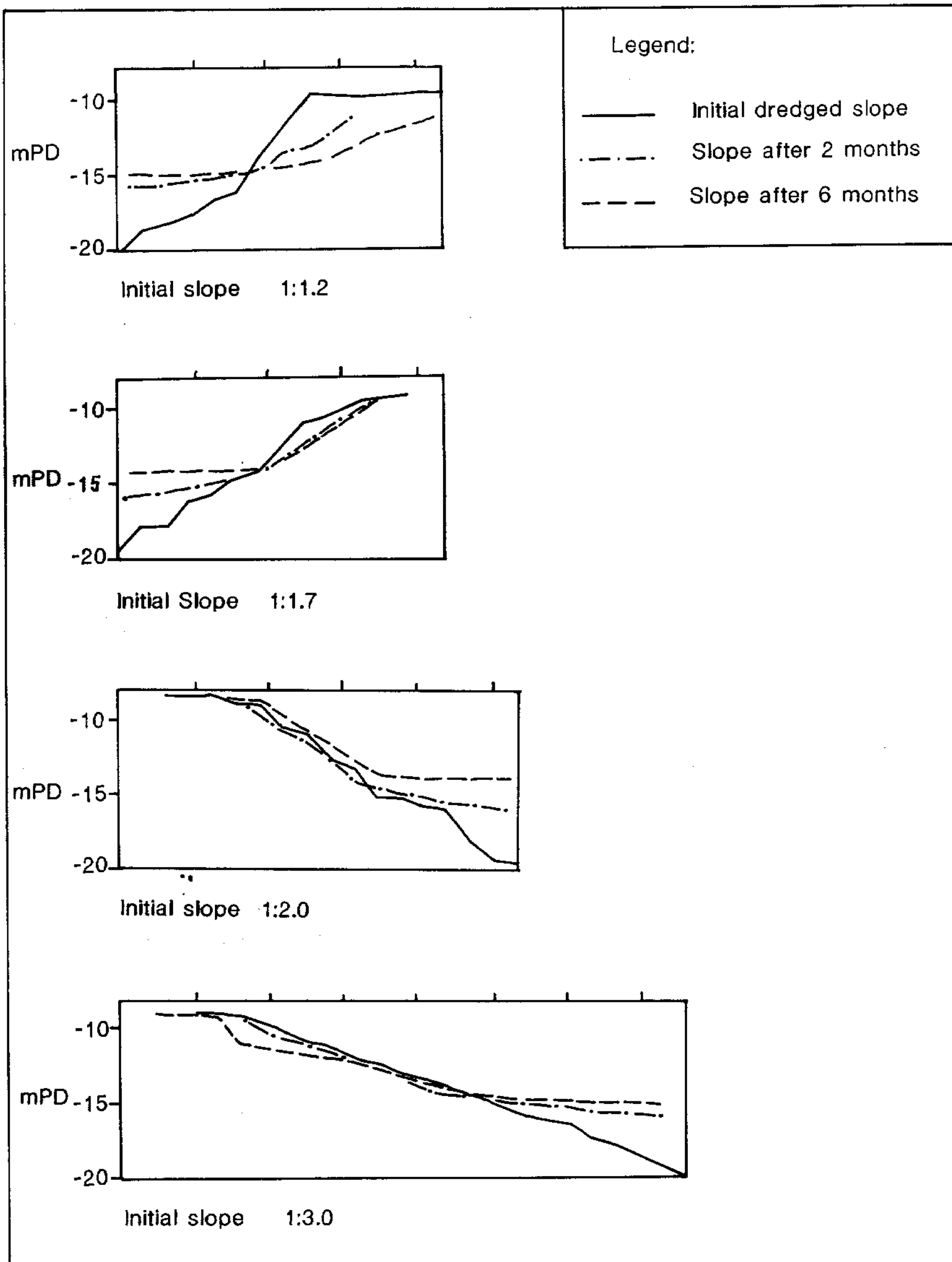

Note: After Ford and Elliot (1965)

Figure 17 - Performance of Slopes Dredged in Seabed Mud, Plover Cove Reservoir

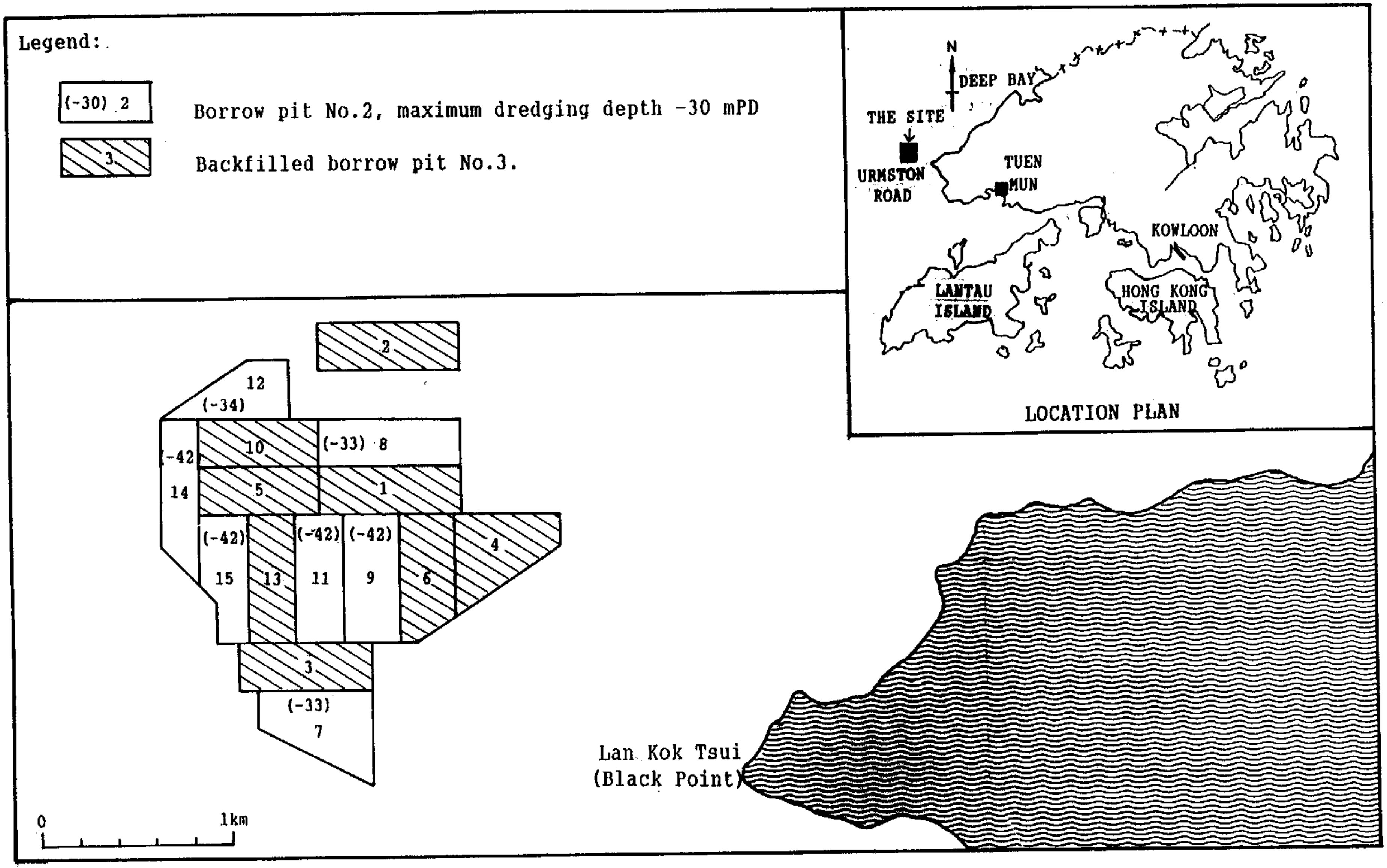

Figure 18 - Location Plan, Urmston Road Borrow Pits

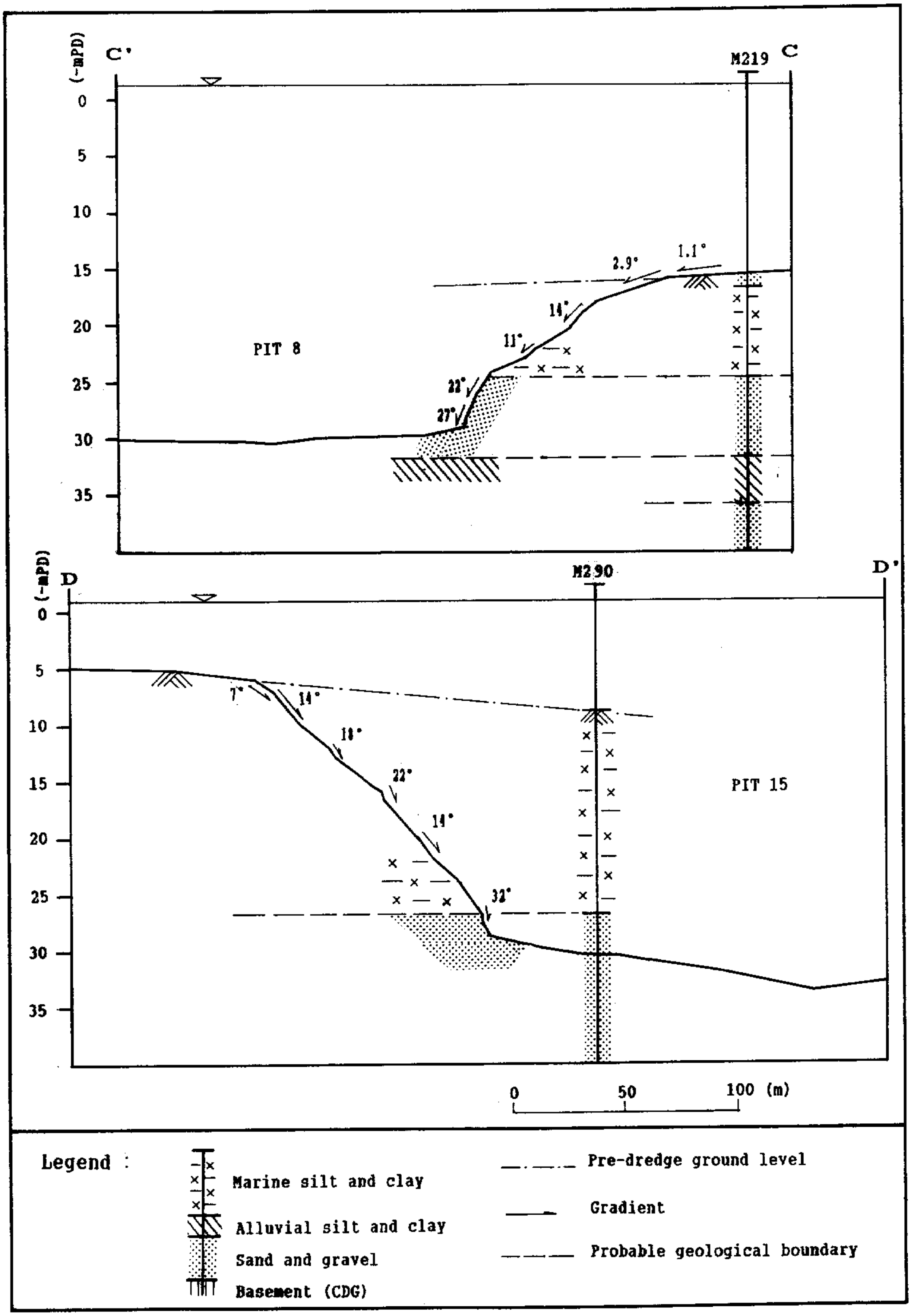

Figure 19 - Urmston Road Borrow Pits, Cross-sections C-C' and D-D'

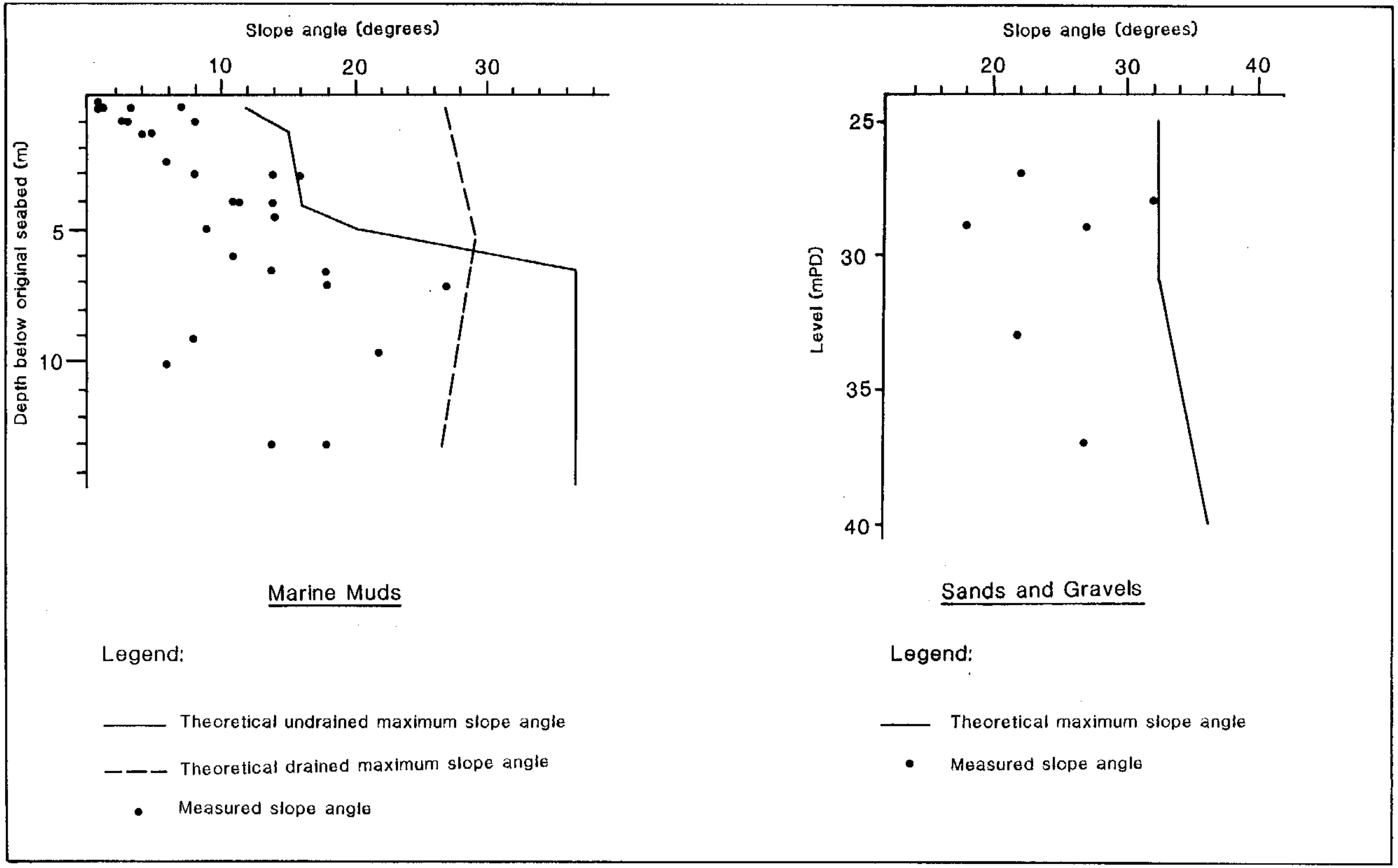

Figure 20 - Urmston Road Borrow Pits, Theoretical and Measured Slope Angles